The Exterior Potential and the Electrocardiogram 7

In Chap. 6 we assumed that the potential outside a nerve cell is zero. This is only approximately true. There is a small potential that can be measured and has clinical relevance. Before a muscle cell contracts, a wave of depolarization sweeps along the cell. This wave is quite similar to the wave along the axon. Measurement of these exterior signals gives us the electrocardiogram, the electromyogram, and the electroencephalogram.

In Sect. 7.1 we calculate the potential outside a long cylindrical axon bathed in a uniform conducting medium. Section 7.2 shows that the exterior potential is small compared to the potential inside the cell if there is enough extracellular fluid so that the outside resistance is low. Section 7.3 uses a model in which the action potential is approximated by a triangular pulse to calculate the potential far from the cell. Section 7.4 generalizes this calculation to the case of a pulse of arbitrary shape.

An unusual feature of heart muscle is that the myocardial cells remain depolarized for 100 ms or so, as described in Sects. 7.5 and 7.6. This means that the potential difference outside the cell is much larger than for other cells, giving rise to the electrocardiogram described in Sects. 7.7 and 7.8. These two sections discuss electrocardiography and some factors that contribute to the signal. They make no attempt to consider advanced techniques such as orthogonal leads that are used to reconstruct the electrical activity of the heart from potential difference measurements on the surface of the body. Rather, they are much closer to the way clinicians think about the electrocardiogram, and they can provide a basis from which to learn more complicated techniques.

Section 7.9 talks about improved models that take into account the interaction between the inside and outside of cells and the anisotropies that exist in tissue resistance. Section 7.10 discusses the problem of stimulation: for measurement of evoked responses, for pacing, and for defibrillation.

Section 7.11 discusses the electroencephalogram.

7.1 The Potential Outside a Long Cylindrical Axon

When studying the action potential in Chap. 6 we assumed that the potential outside the axon is zero. Now we calculate the exterior potential distribution if the axon is in an infinite uniform conducting medium.[1] We will discover that for the case studied here the exterior potential changes are less than 0.1 % of those inside. If the exterior medium is not infinite, the exterior potential changes are larger, as is discussed in Sect. 7.9. This model also applies to a muscle cell that is depolarizing before contraction. We will adapt these results to a group of heart (myocardial) cells that depolarize together, leading to a wave of depolarization propagating through the tissue.

Consider a single axon stretched along the x axis. Divide space into three regions as shown on the left in Fig. 7.1: the interior of the axon (the axoplasm), the axon membrane, and the surrounding medium. Imagine that the current inside the axon is constant to the left of a certain point and zero to the right of that point, as shown on the right in Fig. 7.1b Since the axoplasm obeys Ohm's Law, the interior potential decreases linearly with x as shown in Fig. 7.1a. Where the current is zero, the interior potential does not change. At the point where the interior current falls to zero, conservation of charge requires that the current passes through the membrane and flows in the exterior conducting medium, as stated in Eq. 6.47b. Figure 7.1c shows the axon with current flowing in the left part of the axon and then flowing into the surrounding medium.

Now consider how the current flows in the surrounding three-dimensional medium. Suppose that the surrounding or "outside" medium is infinite, homogeneous and isotropic and has conductivity σ_o. Suppose also that the axon stretched

[1] Other textbooks examine this problem in greater detail (Gulrajani 1998; Malmivuo and Plonsey 1995).

R. K. Hobbie, B. J. Roth, *Intermediate Physics for Medicine and Biology*,
DOI 10.1007/978-3-319-12682-1_7, © Springer International Publishing Switzerland 2015

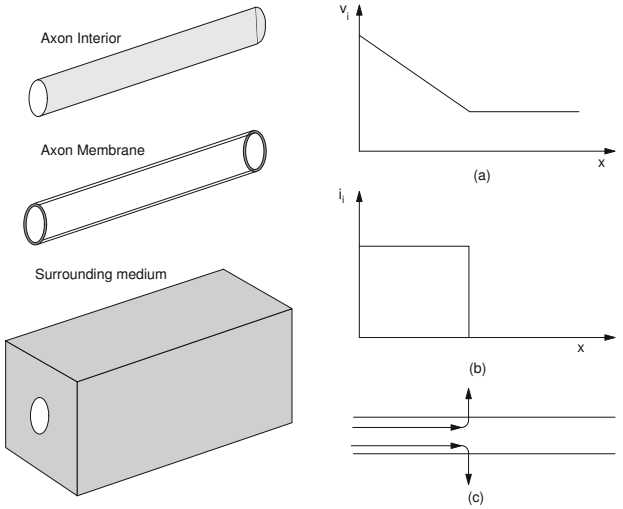

Fig. 7.1 An axon is stretched along the x axis. **a** A plot of a portion of the interior action potential at one instant of time. **b** A plot of the interior current, proportional to the slope of the interior potential because of Ohm's law. **c** Schematic representation of the axon, showing current flowing along the axon and into the exterior conducting medium at the point where the interior current falls to zero

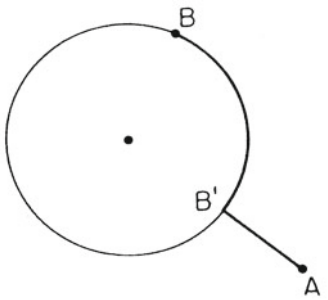

Fig. 7.2 A point current source is at the *center* of a sphere. The path of integration to calculate the potential difference between points A and B goes first from A to B' and then from B' to B

along the x axis is very thin and does not appreciably change the homogeneous and isotropic nature of the extracellular medium, except very close to the x axis. If a current i_o enters the surrounding medium at the origin, the current density **j** is directed radially outward and has spherical symmetry. The current density at distance r has magnitude $j = i_o/4\pi r^2$. The magnitude of the electric field is $E = j/\sigma_o = i_o/4\pi\sigma_o r^2$. This has the same form as the electric field from a point charge, for which the electric field is $E = q/4\pi\epsilon_0 r^2$. We speak of i_o as a *point current source*.

We can use the expression for the electric field to calculate the exterior potential. The point current source is shown as the dot in the center of the sphere in Fig. 7.2. To calculate the potential difference between points A and B, it is easier to integrate Eq. 6.16 along a path from A to B' parallel to the direction of **E**, and then along $B'B$ where the displacement is

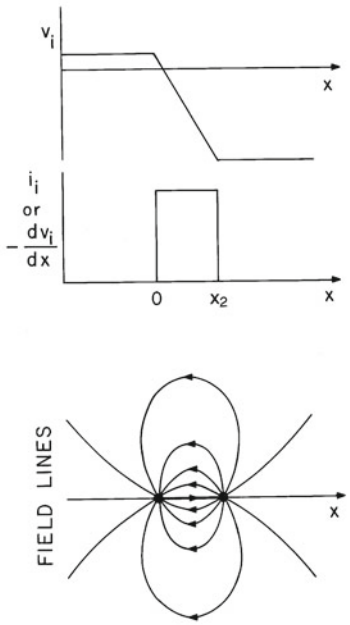

Fig. 7.3 The potential of Fig. 7.1 is extended to the left in a region of constant (depolarized) potential. The interior current is plotted below the potential. The electric field or current-density lines are plotted at the bottom. The current to the right on the axis is current within the axon; the other lines represent current in the exterior conducting medium

always perpendicular to **E**. The potential change along $B'B$ is zero. Therefore,

$$v(B) - v(A) = -\int_{r_A}^{r_B} E_r\, dr = -\int_{r_A}^{r_B} \frac{i_o}{4\pi\sigma_o r^2} dr$$
$$= \frac{i_o}{4\pi\sigma_o}\left(\frac{1}{r_B} - \frac{1}{r_A}\right).$$

Only a difference of potential between two points has meaning. However, it is customary to define the potential to be 0 at $r_A = \infty$ and speak of the potential as a function of position. Then the potential at distance r from a point current source i_o is

$$v(r) = \frac{i_o}{4\pi\sigma_o r}. \tag{7.1}$$

The analogous expression for the potential due to a point charge q is $v(r) = q/4\pi\epsilon_0 r$.

We do not yet have a useful model, because the potential cannot rise forever as we go along the axon to the left. Let us assume that the potential levels off at some point on the left, as shown in Fig. 7.3. (This will turn out to be a very good model for the electrocardiogram, because the repolarization of myocardial cells does not take place for about 100 ms, so the cells are completely depolarized before repolarization begins.) Define the location of the origin so that the depolarization takes place between $x = 0$ and $x = x_2$. The potential

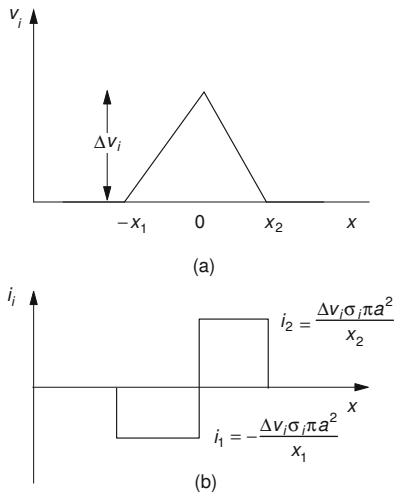

Fig. 7.4 The action potential is approximated by a triangular wave form. In this piecewise-linear approximation, the depolarization and repolarization are both linear. **a** The interior potential. **b** The interior current

change is shown at the top, and the current along the inside of the axon in the middle. The current exists only where there is a voltage gradient between $x = 0$ and $x = x_2$. Its magnitude is $i_i = \Delta v_i / R = \Delta v_i \sigma_i \pi a^2 / x_2$. This current flows out into the surrounding medium at $x = x_2$ and back into the axon at $x = 0$. Such a combination of source and sink of equal magnitude is called a *current dipole*. (A pair of equal and opposite electric charges is called an electric dipole.) The lowest part of the figure shows lines of **j** or **E**. The current is to the right inside the axon (along the axis) and returns outside the axon. The potential at any exterior point is due to two terms: one from the source i_i at $x = x_2$ and the other from the sink $-i_i$ at $x = 0$. If r_2 is the distance from the observation point to x_2 and r_0 is the distance to the origin, then

$$v = \frac{\Delta v_i \sigma_i \, \pi a^2}{4\pi \, \sigma_o x_2} \left(\frac{1}{r_2} - \frac{1}{r_0} \right) = \frac{\Delta v_i \sigma_i a^2}{4\sigma_o x_2} \left(\frac{1}{r_2} - \frac{1}{r_0} \right). \tag{7.2}$$

To estimate the exterior potential from a nerve impulse, we can approximate the action potential by a triangular potential as shown in Fig. 7.4a. The potential is zero far to the left. It rises by an amount Δv_i between $x = -x_1$ and $x = 0$. It falls linearly to zero at $x = x_2$. The current is plotted in Fig. 7.4b. In the region just to the left of the origin it is

$$i_1 = -\frac{\Delta v_i \sigma_i \, \pi a^2}{x_1}. \tag{7.3a}$$

(It is negative because it flows to the left.) To the right of the origin it is

$$i_2 = \frac{\Delta v_i \sigma_i \, \pi a^2}{x_2}. \tag{7.3b}$$

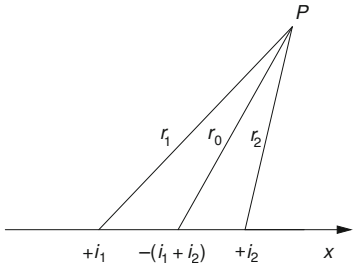

Fig. 7.5 The axon of Fig. 7.4 is stretched along the x axis. There are current sources at $x = -x_1$ and $x = x_2$, and a current sink at the origin. The distances from each source or sink to the observation point P are shown

Figure 7.5 shows the surrounding medium. There is a source of current i_1 at $x = -x_1$, a source i_2 at $x = x_2$, and a sink $-(i_1 + i_2)$ at the origin. The potential at observation point P is calculated by repeated application of Eq. 7.1:

$$v = \frac{1}{4\pi\sigma_o} \left(\frac{i_1}{r_1} - \frac{i_1 + i_2}{r_0} + \frac{i_2}{r_2} \right). \tag{7.3c}$$

Equations 7.3a–7.3c can be combined to give

$$v = \frac{\Delta v_i \sigma_i a^2}{4\sigma_o} \left(\frac{1/x_1}{r_1} - \frac{1/x_1 + 1/x_2}{r_0} + \frac{1/x_2}{r_2} \right). \tag{7.4}$$

Equations 7.3 and 7.4 are valid at any distance from the axon, as long as we can make the piecewise approximation of the action potential shown in Fig. 7.4.

7.2 The Exterior Potential is Small

Let us use Eq. 7.2 for the rising edge of the action potential to estimate the potential outside the axon when it is in an infinite conducting medium. We evaluate Eq. 7.2 close to the surface of the axon where the potential will be largest, say at $x = 0$. In that case r_2 is approximately x_2. However, r_0 is not zero. It can never become smaller than $r_0 = a$, the radius of the axon. (The potential would diverge if the model were extended to $r = 0$.) We will use an approximate value, $r_0 = a$, and call the height of the action potential Δv_i. Then

$$v(0) = \frac{\Delta v_i \sigma_i a^2}{4\sigma_o x_2} \left(\frac{1}{x_2} - \frac{1}{a} \right). \tag{7.5}$$

Since $1/x_2 \ll 1/a$, this becomes

$$v(0) \approx -\frac{\Delta v_i \sigma_i a}{4\sigma_o x_2}. \tag{7.6}$$

Close to $x = x_2$ the potential is

$$v(x_2) = \frac{\Delta v_i \sigma_i a^2}{4\sigma_o x_2} \left(\frac{1}{a} - \frac{1}{x_2} \right) \approx \frac{\Delta v_i \sigma_i a}{4\sigma_o x_2}. \tag{7.7}$$

The potential difference between these two exterior points is

$$\Delta v_o = v(x_2) - v(0) = \frac{\sigma_i}{\sigma_o}\frac{a}{2x_2}\Delta v_i. \tag{7.8}$$

If the conductivities were the same inside and outside, the ratio would be $\Delta v_o/\Delta v_i = a/2x_2$.

The ratio of exterior to interior potential change is proportional to the ratio of the axon radius to the distance along the axon over which the potential changes. From Fig. 6.42 we see that the rising part of the squid action potential has a length $x_2 \approx 1$ cm. If $a = 0.5$ mm (a quite large axon), then the ratio is $1/40$. For a smaller axon, the ratio is even less.

The same result can be obtained by another argument. The resistance between two points is the ratio of the potential difference between the points to the current flowing between them. Inside the axon, **j** and **E** are large because the current is confined to a small region of area πa^2. The resistance inside is $R_i = x_2/\pi a^2\sigma_i$. The same current flows outside, but it is spread out so that **j** and **E** are much less. The resistance between two electrodes in a conducting medium is related to their capacitance (Sect. 6.19). Equations 6.86 and 6.99 can be used to show that two spherical electrodes of radius a spaced distance x_2 apart ($x_2 \gg a$) have a resistance $R_o = 1/2\pi\sigma_o a$. The voltage ratio is

$$\frac{\Delta v_o}{\Delta v_i} = \frac{R_o}{R_i} = \frac{1}{2\pi\sigma_o a}\frac{\pi a^2\sigma_i}{x_2} = \frac{\sigma_i}{\sigma_o}\frac{a}{2x_2},$$

the same result as Eq. 7.8.

7.3 The Potential Far from the Axon

In most cases measurements of the potential are made far from the axon—far compared to the distance the action potential spreads out along the axon. If point P is moved far away, Fig. 7.5 looks like Fig. 7.6. The lines r_1, r_0, and r_2 are nearly parallel. If point P is located at distance r_0 from the origin at angle θ with the x axis, then

$$r_2 \approx r_0 - x_2\cos\theta, \quad r_1 \approx r_0 + x_1\cos\theta. \tag{7.9}$$

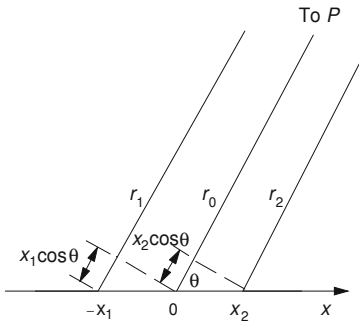

Fig. 7.6 The observation point P is far away compared to distances x_1 or x_2. The *lines* to P are nearly parallel

Consider the potential in Eq. 7.2 due to the leading edge of the action potential. (We will argue later that this is a useful model for the electrocardiogram.) Substituting Eqs. 7.9 in Eq. 7.2 gives

$$v = \frac{\Delta v_i\sigma_i a^2}{4\sigma_o x_2}\left(\frac{1}{r_0[1-(x_2/r_0)\cos\theta]} - \frac{1}{r_0}\right).$$

You can verify by a Taylor's-series expansion or long division that

$$\frac{1}{1-x} = 1 + x + \cdots, \tag{7.10}$$

so that

$$v = \frac{\Delta v_i\sigma_i a^2}{4\sigma_o r_0^2}\cos\theta. \tag{7.11}$$

This is a very important result that will form the basis for our model of the electrocardiogram:

1. The exterior potential v depends on Δv_i but not on x_2, the length of the depolarization region. This is because increasing x_2 decreases the strength of the current at the same time that it increases v because the source and sink are further apart.
2. The potential falls off as $1/r^2$ instead of $1/r$ as it would from a point source.
3. The potential varies with angle, being positive to the right of the transition region and negative to the left.

It is convenient to define a vector **p** that points along the axon in the direction of the advancing depolarization wave front (the region along the axon where the potential rises). It is called the *activity vector* or *current-dipole moment* for reasons discussed shortly. Its magnitude is

$$p = \pi a^2\sigma_i\,\Delta v_i. \tag{7.12}$$

The exterior potential is then (dropping the subscript on **r**)

$$v = \frac{\mathbf{p}\cdot\mathbf{r}}{4\pi\sigma_o r^3}. \tag{7.13}$$

Vector **p** has units of A m. Its magnitude (apart from the conductivity) is the product of the cross-sectional area of the axon and the difference in potential along the axon between the resting and completely depolarized regions. It is called the current-dipole moment because it is the product of the current and the separation of the source and sink. (The electric-dipole moment is the product of the magnitude of the charges and their separation, with units C m.)

Equation 7.11 can also be written in the form

$$v(r) = \frac{\pi a^2\cos\theta}{r^2}\frac{1}{4\pi}\frac{\sigma_i}{\sigma_o}\Delta v_i. \tag{7.14}$$

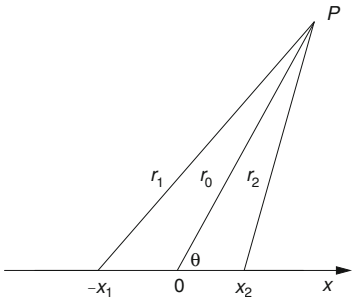

Fig. 7.7 When the observation point is not so far away, or when a complete nerve impulse is being considered, the law of cosines must be used to relate r_1 and r_2 to r_0

The quantity $\pi a^2 \cos\theta / r^2$ is $\Delta\Omega$, the *solid angle*[2] subtended at the observation point by a cross section of the axon where the potential changes. The quantity 4π is the maximum possible solid angle. In terms of the solid angle

$$v = \frac{\Delta\Omega}{4\pi} \frac{\sigma_i}{\sigma_o} \Delta v_i . \tag{7.15}$$

Now consider an entire pulse, one where the potential rises and then returns to the resting value. If the approximation of Eq. 7.10 is applied to Eq. 7.4, the result vanishes. It is necessary to make a more accurate approximation, one that takes into account the fact that the vectors $\mathbf{r}_1$, $\mathbf{r}_0$, and $\mathbf{r}_2$ are not exactly parallel. Figure 7.7 shows the geometry. We use the law of cosines to write [remember that $\cos(\pi - \theta) = -\cos\theta$]

$$r_1 = r_0 \left[1 + (2x_1/r_0)\cos\theta + x_1^2/r_0^2 \right]^{1/2},$$

$$r_2 = r_0 \left[1 - (2x_2/r_0)\cos\theta + x_2^2/r_0^2 \right]^{1/2}.$$

When these are inserted in Eq. 7.4 and a Taylor's-series expansion is done to second order in both x_1/r_0 and x_2/r_0, the result is

$$v = \frac{2\pi a^2}{4\pi r^3} \frac{\sigma_i}{\sigma_o} \frac{\Delta v_i (x_1 + x_2)}{2} \frac{3\cos^2\theta - 1}{2}. \tag{7.16}$$

The constants have been arranged to show that the term $\Delta v_i (x_1 + x_2)/2$ is the area under the impulse when v is plotted as a function of x. The angular factor as written with its factor of 2 in the denominator is tabulated in many places as the *Legendre polynomial* $P_2(\cos\theta)$.[3] The exterior potential

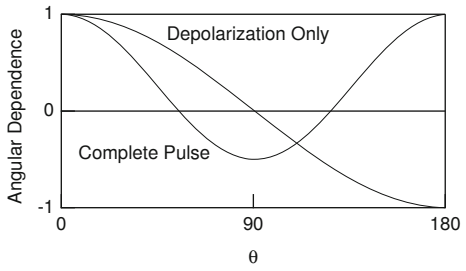

Fig. 7.8 Plot of the angular dependence of the potential from the entire impulse, Eq. 7.16

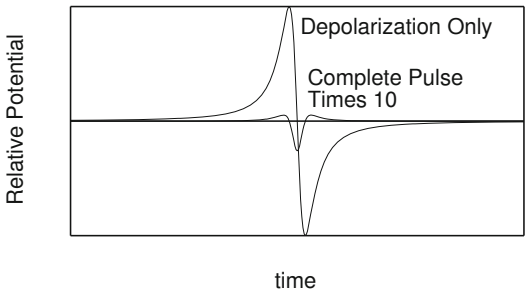

Fig. 7.9 The potential far from the axon as a function of time as an impulse travels from left to right along the axis. The potential from the complete pulse has been multiplied by a factor of 10 in order to show it

now falls off more rapidly with distance, as $1/r^3$. The angular dependence, shown in Fig. 7.8, is symmetric about $\pi/2$. This shows the angular dependence as one moves around the impulse at a constant distance from it.

This is a very different situation and a very different curve from the potential measured at a fixed point outside the axon as an impulse travels past. In the latter case r as well as θ is changing. This behavior is discussed in Problems 8 and 9. The results are shown in Fig. 7.9. The potential from the depolarization is biphasic; that from the complete pulse is triphasic, being positive, then negative, then positive again.

For a single axon in an ionic solution the exterior conductivity is usually higher than in the axon, so $\sigma_i/\sigma_o = 0.2$. The conductivity of tissue is considerably less than the conductivity of an ionic solution, and the ratio becomes greater than one. For the electrocardiogram it will be more appropriate to use $\sigma_o = 0.33\,\mathrm{S\ m^{-1}}$ (muscle) or $0.08\,\mathrm{S\ m^{-1}}$ (lung), in which case σ_i/σ_o is 6 or 25. We will use an approximate value of 10.

7.4 The Exterior Potential for an Arbitrary Pulse

We have derived the results of the previous sections for an action potential that varies linearly during depolarization and repolarization, a piecewise-linear approximation. In general

[2] The solid angle is defined in Appendix A.

[3] You can learn more about Legendre polynomials in texts on differential equations or, for example, in Harris and Stocker (1998). See also Eq. 7.29.

the action potential does not have sharp changes in slope. We will now consider the general case and find that the results are very similar. For depolarization alone, we will again have a potential depending on the dipole moment. For a complete pulse the potential will depend on the area under the pulse curve.

Again, the axon is stretched along the x axis in an infinite, homogeneous conducting medium. Consider a small segment of axon between x and $x + dx$. If the current entering this segment at x is greater than the current leaving at $x + dx$, the difference must flow into the exterior medium. From Eq. 6.47b,

$$di_o = -di_i = -\frac{\partial i_i(x,t)}{\partial x}dx.$$

We can write Ohm's law for the axoplasm as

$$i_i(x,t) = -\pi a^2 \sigma_i \frac{\partial v_i}{\partial x}. \tag{7.17}$$

The current into the exterior medium from length dx of the axon is

$$di_o = \pi a^2 \sigma_i \frac{\partial^2 v_i}{\partial x^2}\, dx. \tag{7.18}$$

It is proportional to the derivative of the current along the axon with respect to x and therefore to the second derivative of the interior potential with respect to x. A small current source di_o generates a potential dv at some point in the exterior medium given by

$$dv = \frac{di_o}{4\pi\sigma_o r}. \tag{7.19}$$

If the radius of the axon stretched along the x axis is very small, the axon's influence can be replaced by a current distribution $di_o(x)$ along the x axis. The potential at any point $\mathbf{R}$ is obtained by integrating Eq. 7.19:

$$v(\mathbf{R}) = \int \frac{di_o}{4\pi\sigma_o r}. \tag{7.20}$$

Vector $\mathbf{R}$ specifies the point at which the potential is measured, and r is the distance from the measuring point to the point on the x axis where di_o is injected, as shown in Fig. 7.10. Combining this with Eq. 7.18 gives

$$v(\mathbf{R}) = \int \frac{\pi a^2 \sigma_i}{4\pi\sigma_o} \frac{\partial^2 v_i}{\partial x^2} \frac{1}{r}\, dx. \tag{7.21}$$

Although it is difficult to integrate Eq. 7.21 analytically, the integration can be done numerically. Figure 7.11 shows a computer program to carry out this integration for a crayfish lateral giant axon immersed in sea water. The axon radius is 60 μm. The conductivity ratio is $\sigma_i/\sigma_o = 0.2$. The action potential was measured by Watanabe and Grundfest (1961). Clark and Plonsey (1968) showed that it could be well represented by a sum of three Gaussians, with $v_i = 0$ taken to be

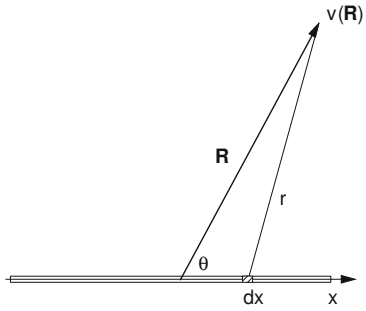

Fig. 7.10 The potential $v(\mathbf{R})$ is obtained by integrating the potential due to current di_o from each element dx of the cell

the resting value. Since only $\partial^2 v_i/\partial x^2$ enters into Eq. 7.21, the reference level does not matter. The representation (with v in mV and x in mm) is

$$v_i(x) = 51e^{-[(x-5.4)/1.25]^2} + 72e^{-[(x-6.6)/1.876]^2} + 18e^{-[(x-8.6)/3.003]^2}. \tag{7.22}$$

This function corresponds to an impulse traveling to the left. It can be differentiated to obtain an analytic expression for $\partial^2 v_i/\partial x^2$. If the potential is being measured at exterior point (x_0, y_0), the value of r which is used in Eq. 7.21 is $r = \left[(x - x_0)^2 + y_0^2\right]^{1/2}$. The program allows four values of y_0 to be used. The smallest is taken to be a, the radius of the axon.

The results of calculating the exterior potential at $y_0 = a$ are shown in Fig. 7.12. The interior potential, shown in (a), has a peak value of 114 mV. The potential on the surface of the axon (b) ranges from $+0.04$ to -0.07 mV. In general the exterior potential is less than 0.1 % of the interior potential. (This would be different if the extracellular fluid were not infinite.) The original calculation by Clark and Plonsey used much different mathematical techniques (see Problem 30); however, the results are very similar. The results of their more accurate calculation are plotted in Fig. 7.13.

The approximation that the observer is far from the axon can also be applied to the general case. The physics is exactly the same as in the previous section for the triangular pulse, except that now the pulse has an arbitrary shape so current passes through the membrane at all points along the axon where the second derivative is nonzero. The calculation requires making the same type of approximations in order to evaluate the integral (Eq. 7.21). Referring to Fig. 7.10, we again use the law of cosines to write

$$r(x) = R\left[1 - 2(x/R)\cos\theta + x^2/R^2\right]^{1/2}.$$

We need to use this in Eq. 7.21. As in the previous section, we make a Taylor's-series expansion of $1/r$. To second order

```
//program ClarkAndPlonsey;
/*This program integrates our approximate
equation for the extracellular potential.
Original calc. by J. Clark and R. Plonsey,
The extracellular potential field of the
single active nerve fiber in a volume
conductor. Biophys. J. 8:842-864 (1968)*/
/*The nerve pulse is a series of Gaussians
used by Clark and Plonsey to fit data of
Watanabe and Grundfest, J. Gen. Physiol.
45:267 (1961)*/
/*This program uses Romberg integration
function qromb, from the Numerical Recipes
in C, 2nd ed.*/

#include<stdio.h>
#include<stdlib.h>
#include<math.h>
#include "nr.h" //N.R. in C header file

/*Global Variables*/
double x0,y0; //coordinates of obs point

float f(float x)
{
/*Calculates integrand d2v/dx2 div by r
   Uses common variables x0 , y0--
Observation point in meter*/
double   xx, r, d2v, temp;
d2v = 0;
xx = (x-0.0054)/1.25e-3;
temp = (2*51/(1.25e-3*1.25e-3))
   *exp(-(xx*xx));
d2v = d2v+temp*(2*xx*xx-1);
xx = (x-0.0066)/1.876e-3;
temp = (2*72/(1.876e-3*1.876e-3))
   *exp(-(xx*xx));
d2v = d2v+temp*(2*xx*xx-1);
xx = (x-0.0086)/3.003e-3;
temp = (2*18/(3.003e-3*3.003e-3))
   *exp(-(xx*xx));
d2v = d2v+temp*(2*xx*xx-1);
r = sqrt((x0-x)*(x0-x)+y0*y0);
return d2v/r;
}

void main()
{
const
   double SigRatio = 0.2,
   //Interior/exterior conductivity
   a = 6.0e-5;  //axon radius in m
float
   xstart, xfinish,//limits of int.;
double
   y[4],//Calculate at four distances
   potential, xx  //Exterior potential
  Transmemb;   //Transmembrane potential
int i;
FILE *ofp;        //Outputfile Pointer
if (!(ofp = fopen("Plonsey.out","w")))
//Open output file
{
   printf("cannnot open output file\n");
   exit(1);
}
xstart = 0.0;
xfinish = 0.02;
fprintf(ofp,"    x   \t    v   ");
printf("     x          v    ");
for (i=0; i<4; i++)
{
   y[i] = pow(2,i)*a;
   fprintf(ofp,"\t%9.3e",y[i]);
   printf(" %9.3e ",y[i]);
}
fprintf(ofp,"\n\n");
printf("\n\n");
for(x0 = 0.001; x0 < 0.012; x0 += 0.00025)
{
   xx = (x0-0.0054)/1.25e-3;
   Transmemb = 51*exp(-xx*xx);
   xx = (x0-0.0066)/1.876e-3;
   Transmemb = Transmemb+72*exp(-xx*xx);
   xx = (x0-0.0086)/3.003e-3;
   Transmemb = Transmemb+18*exp (-xx*xx);
   fprintf(ofp,"%9.3e\t%10.3e",x0,Transmem
b);
   printf("%9.3e %10.3e ",x0,Transmemb);
   for (i=0; i<4 ; i++)
   {
      y0 = y[i];
      Integral = qromb(f,xstart,xfinish);
//N.R. in C function Call
      potential=Integral*a*a*SigRatio/4.0;
      fprintf(ofp,"\t%10.3e",potential);
      printf("%10.3e ",potential);
   }
   fprintf(ofp,"\n");
   printf("\n");
   }
fclose(ofp);
}
```

Fig. 7.11 The computer program used to calculate the exterior potential by integrating Eq. 7.21 for the problem first solved by Clark and Plonsey (1968). The program uses Romberg integration procedure `qromb` from Press et al. (1992)

the result is

$$\frac{1}{r} \approx \frac{1}{R}\left(1 + \frac{x}{R}\cos\theta + \frac{1}{2}\frac{x^2}{R^2}(3\cos^2\theta - 1)\right). \tag{7.23}$$

The expression for $v(\mathbf{R})$ becomes

$$v(R) = \frac{\pi a^2 \sigma_i}{4\pi\sigma_o}\left[\frac{1}{R}\int_{x_1}^{x_2}\frac{\partial^2 v_i}{\partial x^2}\,dx + \frac{\cos\theta}{R^2}\int_{x_1}^{x_2}\frac{\partial^2 v_i}{\partial x^2}x\,dx + \frac{3\cos^2\theta - 1}{2R^3}\int_{x_1}^{x_2}\frac{\partial^2 v_i}{\partial x^2}x^2\,dx\right]. \tag{7.24}$$

There are three integrals that we must evaluate. Take limits of integration x_1 and x_2 to be points where $\partial v_i/\partial x = 0$. The first integral is $\partial v_i/\partial x$ which vanishes at the end points. The second integral can be integrated by parts. Since $\partial v_i/\partial x = 0$ at the end points the second integral is $v_i(x_1) - v_i(x_2)$. The third integral is integrated by parts twice and is

$$\int_{x_1}^{x_2}\frac{\partial^2 v_i}{\partial x^2}x^2\,dx = \left[x^2\frac{\partial v_i}{\partial x}\right]_{x_1}^{x_2} - 2\left[x v(x)\right]_{x_1}^{x_2} + 2\int_{x_1}^{x_2} v_i(x)\,dx. \tag{7.25}$$

The first term of this vanishes because of the way the end points were chosen.

We now apply these results to Eq. 7.24 in two cases. The first is the case of depolarization only, which is useful in considering the electrocardiogram. Set up the coordinate system so the origin is someplace in the impulse where $\partial v_i/\partial x = 0$. The total change in v_i is Δv_i. Then $x_1 = 0$, $v_i(x_1) = \Delta v_i$, $v_i(x_2) = 0$. The first nonvanishing term of Eq. 7.24 requires only the second integral:

$$v(\mathbf{R}) = \frac{\pi a^2 \sigma_i}{4\pi\sigma_o}\frac{\cos\theta}{R^2}\Delta v_i. \tag{7.26}$$

We obtained this result in a special case as Eq. 7.11.

In the second case we consider the complete pulse, and we take x_1 to the left of the pulse and x_2 to the right. The first integral in Eq. 7.24 still vanishes. Now the second integral also vanishes because $v_i(x_1) = v_i(x_2) = v_{\text{rest}}$ and $\Delta v_i = 0$. It is necessary to use the third integral, Eq. 7.25. The first term in Eq. 7.25 vanishes. The second and third terms must be considered together. Rewrite the potential in terms of departures from the resting potential: $v_i(x) = v_{\text{rest}} + v_{\text{depol}}(x)$.

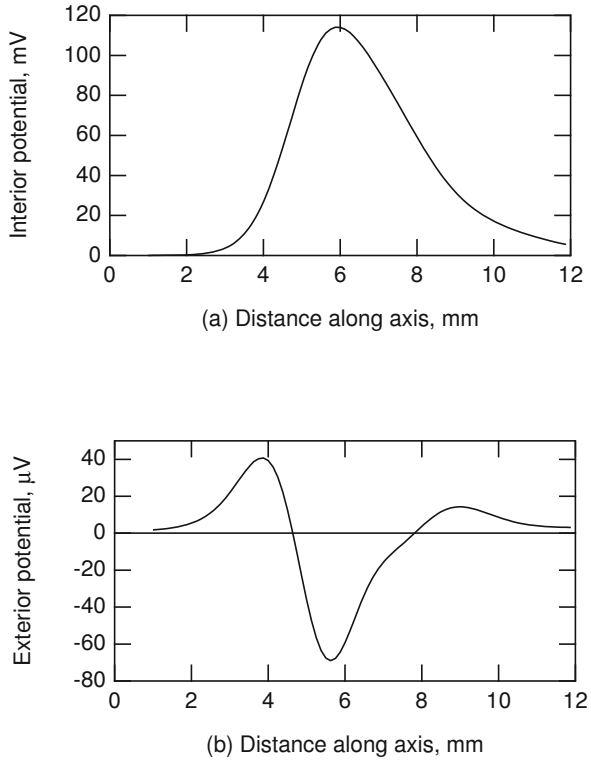

Fig. 7.12 **a** The transmembrane potential used for the calculation in the program of Fig. 7.11. The impulse is traveling to the *left*. **b** The exterior potential along the axon calculated by the program for $y_0 = a$

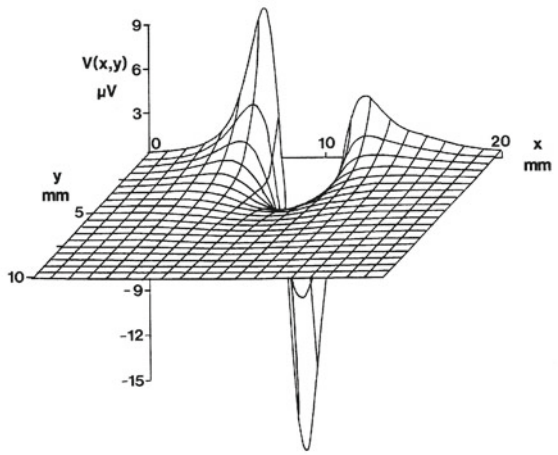

Fig. 7.13 The exterior potential for the same problem calculated using the more accurate method of Clark and Plonsey (1968). The smallest distance from the axon is $y = 0.5$ mm

The second term in Eq. 7.25 is $-2v_{\text{rest}}(x_2 - x_1)$. The third term of Eq. 7.25 is

$$2\int_{x_1}^{x_2} v_{\text{depol}}(x)\,dx + 2(x_2 - x_1)v_{\text{rest}}.$$

Adding these gives

$$v(\mathbf{R}) = \frac{2\pi a^2 \sigma_i}{4\pi\sigma_o}\frac{1}{R^3}\frac{3\cos^2\theta - 1}{2}\int_{x_1}^{x_2}[v_i(x) - v_{\text{rest}}]\,dx. \tag{7.27}$$

Again, we saw a special case of this as Eq. 7.16.

Note the progression in these results. When we are looking at one corner of a depolarization pulse, we have a current source or sink, and the potential is proportional to $1/R$ (Eq. 7.1). We do not find this situation in physiology because the potential would have to keep rising forever. When we consider the entire depolarization portion of the wave form, the potential is proportional to $1/R^2$, as in Eqs. 7.11 or 7.26 (We will find that this is a good model for the electrocardiogram because the repolarization does not commence until the entire heart is depolarized[4]). When the entire pulse is considered, the potential is proportional to $1/R^3$ as in Eq. 7.16 or 7.27. This is a good model for nerve conduction. The potential is considerably less in this case because of the $1/R^3$ dependence.

This is an example of a technique called a *multipole expansion*. Generally, defining $\xi = x/R$, one can make the expansion

$$\frac{1}{(1 - 2\xi\cos\theta + \xi^2)^{1/2}} = P_0 + \xi P_1 + \xi^2 P_2 + \xi^3 P_3 + \cdots, \tag{7.28}$$

where the P_n are functions of $\cos\theta$ and are called Legendre polynomials. The first few Legendre polynomials are

$$\begin{aligned} P_0 &= 1, \\ P_1 &= \cos\theta, \\ P_2 &= \tfrac{1}{2}(3\cos^2\theta - 1), \\ P_3 &= \tfrac{1}{2}(5\cos^3\theta - 3\cos\theta). \end{aligned} \tag{7.29}$$

All of these calculations are based on a model in which the current flows parallel to the axis of the axon, passes through the membrane, and then returns in the extracellular conducting medium. This model is called the *line approximation*. It is, of course, impossible for current inside the axon to pass out through the membrane if it always flows parallel to the axis of the axon. It is possible to do an exact calculation in which **j** has a radial component as well as one parallel to the axis of the axon. (See Sect. 7.9 for a description of how this is done.) Trayanova et al. (1990) have compared the exact solution with two approximations, one of which is the line approximation. The line approximation is quite good if the radius of the axon is much smaller than the distance along the axon over which the depolarization takes place.

[4] This is not strictly true. Atrial repolarization begins before the ventricular depolarization is complete.

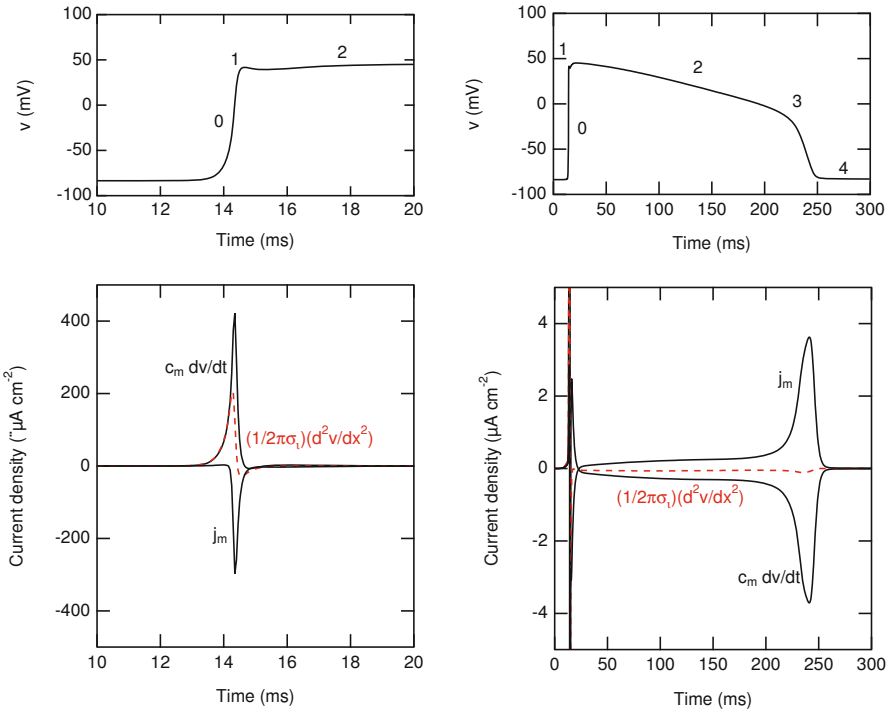

Fig. 7.14 Depolarization and repolarization of cardiac cells based on a model by Luo and Rudy (1994). Panels on the left show the depolarization. Panels on the right show the entire action potential. Note the factor of 100 change in scale of the current density on the lower two panels. Electrotonus (the dashed line) is important during depolarization but is almost nonexistent during repolarization. Compare this with Fig. 6.42. The calculations were performed by Sunil Kandel

7.5 Electrical Properties of the Heart

We saw in Chap. 1 that the heart is divided into a right side and a left side (see Fig. 1.34). Each side consists of an *atrium* and a *ventricle*. The ventricles are primarily responsible for pumping the blood. They are relatively large chambers with thick walls. The smaller atria contract first. The atria fill the ventricles with blood before the ventricles contract. The two chambers on each side are connected by one-way valves: the *tricuspid valve* on the right and the *mitral valve* on the left, so that blood cannot regurgitate back into the atrium when a ventricle contracts.

The right and left atria are electrically connected: if the right atrium contracts, so does the left atrium. The right and left ventricles are similarly connected. The electrical connection between the atria and the ventricles occurs only at the AV node, as discussed below.

There are many similarities between myocardial cells and nerve cells: a membrane separates extracellular and intracellular fluids; the concentrations of the principal ions are about the same; except for a small amount of charge on the membrane, the extracellular and intracellular fluids are electrically neutral; and selective ion channels are responsible for the initiation and propagation of the action potentials. There are also major differences: myocardial cells in mammals are about 100 μm long and 10 μm in diameter. The interiors of neighboring cells are connected through *gap junctions*, so current and ions flow directly from one cell to another (Delmar and Sorgen 2009). This continuum of cells is called a *syncytium*. There are also important differences in the details of the ion currents. We continue for now to use the simple model of long, one-dimensional cells. Refinements to this model are discussed in Sect. 7.9.

In the resting state, the potential inside an atrial cell is about −70 mV, while that in a ventricular cell is about −85 mV. When a cell depolarizes, the action potential lasts for 100–300 ms, depending on the species. A "typical" action potential is shown in Fig. 7.14. There are variations in pulse shape between species and also in different parts of the heart. The initial rapid depolarization is caused by an inward sodium current (phase 0 on the curve) and takes about 1 ms. This is sometimes followed by a rapid fall (phase 1) not prominent in Fig. 7.14, caused by a transient outward potassium current. This current is small in *endocardium* (near the inside of the heart) but is prominent enough in the *epicardium* (outer layers of the heart) so that there can be a "spike and dome" shape to the potential (George 2009). This is followed by a Ca^{2+} influx that maintains the plateau (phase 2) of the action potential. The "slow" potassium channels

finally open (Oudit and Backx 2004), and potassium efflux causes repolarization (phase 3). During phase 4 the original ion concentrations are restored.

The heart can beat in isolation. If it is removed from an animal and bathed in nutrient solution, it continues to beat spontaneously. With each beat, a wave of depolarization sweeps over the heart, and it contracts. The wave is initiated by some specialized fibers located in the right atrium called the *sinoatrial node* (SA node). As was mentioned in Sect. 6.18, the SA node does not have the usual sodium channels, and the depolarization is due to calcium. The shape of the SA node potential is much more like Fig. 6.48 than Fig. 7.14. In humans the SA node fires about 60–100 times per minute; this rate is increased by the *sympathetic* nerves to the heart (which release *norepinephrine*) and decreased by the *parasympathetic* nerves (which release *acetylcholine*). Devices that produce such periodic firing are common in physics and engineering. They are called free-running relaxation oscillators.

Figure 7.15 shows how the depolarization progresses through the heart. Once the SA node has fired, the depolarization sweeps across both atria (a, b). When the atria are completely depolarized (c) there is no depolarization wavefront. The atria are separated from the ventricles by fibrous connective tissue that does not transmit the impulse. The only electrical connection between the atria and the ventricles is some conduction tissue called the *atrioventricular node* (AV node). After passing through the AV node, the depolarization spreads rapidly over the ventricles through the *conduction system*—a set of specialized muscle cells on the inner walls of the ventricles—(d, e), and finally through the myocardium of each ventricle to the outer wall (e, f, g). The conduction system consists of the *common bundle* (or *bundle of His*), the *left and right bundles,* and the fine network of *Purkinje fibers*. The AV node will spontaneously depolarize at a rate of about 50 beats per minute; it usually does not because it is triggered by the more rapid beating of the atria. In well-trained athletes, the resting pulse rate can be so low that the AV node fires spontaneously, giving rise to what are called nodal escape beats. These are physiologic and no cause for concern.

There is a difference between depolarization, which propagates as a wave, and repolarization, which is a local phenomenon. Sodium conductance increases as the transmembrane potential rises during depolarization. As the potential rises at some point on the advancing wave front, electrotonus increases the potential further along the cell, as can be seen in the left panels of Fig. 7.14, where the contribution from electrotonus is shown by the dashed line. This causes the sodium conductance to rise at that point, resulting in the propagation of the signal at speeds of about $0.2 - 0.5$ m s^{-1}. During repolarization electrotonus contributes almost nothing to the repolarization, as can be seen in the panels on the right (note the factor of 100 difference in the current density).

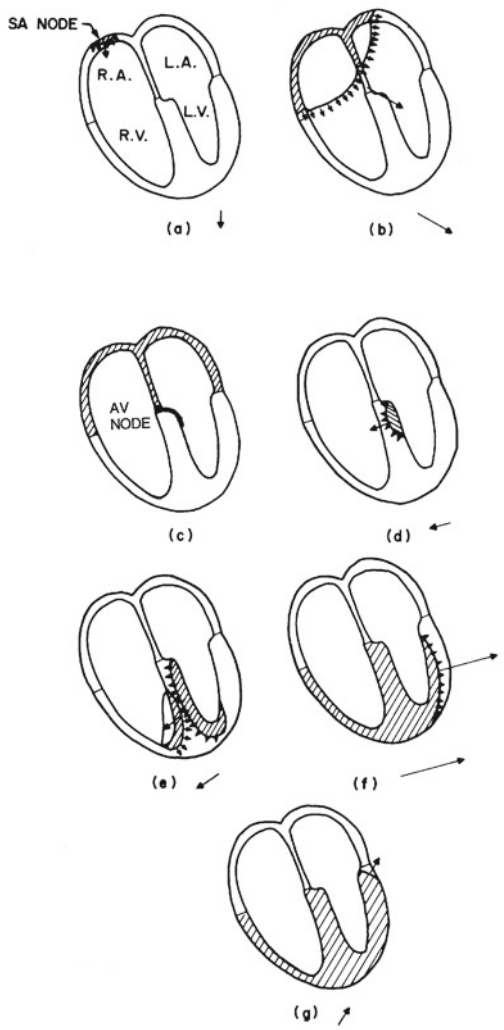

Fig. 7.15 The wave of depolarization sweeping over the heart. Atrial and ventricular muscle are not connected except through the AV node. **a** Depolarization beginning at the SA node. **b** Atria nearly depolarized. **c** The AV node is conducting. **d** Beginning of depolarization of the left ventricle. **e**, **f** Continuing ventricular depolarization. **g** Ventricular depolarization nearly complete. (Reprinted with permission from Hobbie 1973, Copyright © 1973, American Association of Physics Teachers)

Normally, depolarization progresses through the myocardium in an orderly fashion (Fig. 7.15). It is followed by repolarization, and after a brief *refractory period* the heart is ready to beat again. During the refractory period the cells do not respond to a stimulus. It is possible in abnormal situations for a wave of depolarization to travel in a closed path through the myocardium. This closed path, called a *reentrant circuit*, can surround an obstacle such as scar tissue, the aorta, or the pulmonary artery. It can also surround an area that simply has different conduction properties. If the time to travel around the reentrant circuit is greater than the refractory period, the

wave can continue to travel on the closed path. Reentrant excitation is thought to be responsible for several kinds of heart disease, including most life-threatening *ventricular tachycardias* (rapid heart rate). Another type of reentrant excitation is spiral waves that occur because of the nonlinear nature of the myocardium (Gray 2009; Such nonlinear behavior will be discussed in Chap. 10). It is also possible for a reentrant wave to leave behind a refractory state that blocks normal conduction.

7.6 The Current-Dipole Vector of the Heart as a Function of Time

Each myocardial cell depolarizes and repolarizes during the cardiac cycle. These cells are short—about 100 μm in length—but are interconnected. We apply our axon model by noting that a current i_i flows within each cell during depolarization and a return current, which could be ignored in our axon model, flows in the surrounding tissue. We assume that each cell as it depolarizes has a current dipole moment, and that these can be summed.

The total current-dipole vector at any instant is then the sum of the vectors for all the cells in the heart. This section considers how the total current-dipole vector changes with time as the myocardium depolarizes and then repolarizes. Initially, all the cells are completely polarized (resting) and there is no net dipole moment. The cells begin to depolarize near the SA node, and a wave of depolarization sweeps across the atria. For each myocardial cell, the dipole vector points in the direction that the wave of depolarization is traveling[5] and moves along the cell with the depolarization wave. These vectors for all the cells that are depolarizing constitute an advancing wave that moves across the heart.

The potential at the point of observation can be calculated by applying Eq. 7.13 for each cell. Vector **r** is the vector from the cell to the point of observation and is different for each cell. However, we will assume for now that the observation point is so far from the heart that all points in the myocardium are nearly equidistant from it. This is a terrible assumption; later we will be more realistic. It allows us to speak of the *instantaneous total current dipole moment*, which is the sum of the dipole moments of all depolarizing cells at that instant.

The locus of the tip of the total dipole moment during the cardiac cycle is shown in Fig. 7.16 for a typical case. The x axis points to the patient's feet, the y axis to the patient's left, and the z axis from back to front. The small loop labeled P occurs during atrial depolarization. The loop labeled QRS is the result of ventricular depolarization. Ventricular repolarization gives rise to the "T wave." Atrial repolarization is masked by ventricular depolarization. A plot of the x, y, and z components of **p** is shown in Fig. 7.17. These components are typical; there can be considerable variation in the directions of the loops in Fig. 7.16.

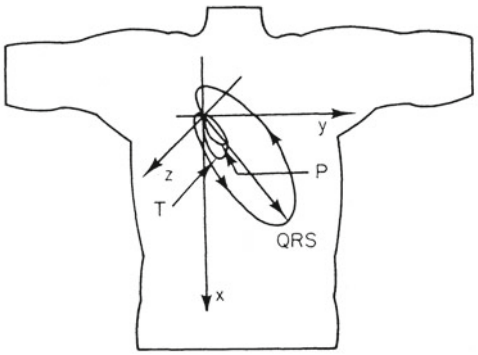

Fig. 7.16 The locus of the tip of the total current-dipole vector during the cardiac cycle. The z axis is perpendicular to the x and y axes and the subject's chest and comes out of the page

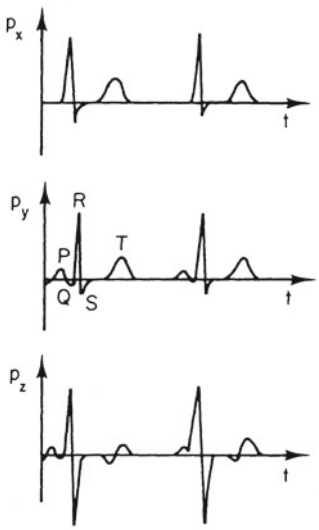

Fig. 7.17 The three components of the total current dipole vector **p** as a function of time

7.7 The Electrocardiographic Leads

We turn next to how the electrocardiographic measurements are made. We model the torso as an infinite homogeneous conductor and continue to assume that every myocardial cell

[5] If one takes into account the anisotropies in the conductivities of myocardial tissue discussed in Sect. 7.9, the depolarization does not travel in the direction that **p** points. We ignore this for now.

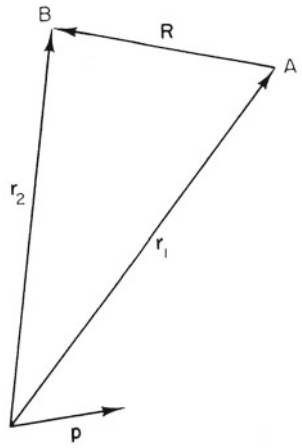

Fig. 7.18 Geometry for calculating the potential difference due to **p** between points *A* and *B*

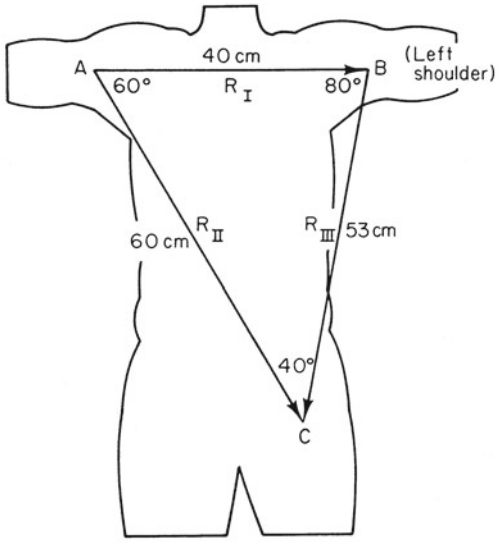

Fig. 7.19 Vectors connecting the three electrodes for a typical patient. The limbs are extensions of the leads of the electrocardiograph machine

is the same distance from each electrode. Both assumptions are wrong, of course, and later we will improve upon them.

The potential at **r** from a current dipole **p** is given by Eq. 7.13. The potential difference between two points at positions $\mathbf{r}_1$ and $\mathbf{r}_2$, each at a distance r from the dipole, is therefore (see Fig. 7.18)

$$v(\mathbf{r}_2, \mathbf{r}_1) = \frac{\mathbf{p} \cdot (\mathbf{r}_2 - \mathbf{r}_1)}{4\pi\sigma_o r^3}.$$

Denoting $\mathbf{r}_2 - \mathbf{r}_1$ by **R**, we have

$$v = \frac{\mathbf{p} \cdot \mathbf{R}}{4\pi\sigma_o r^3}. \tag{7.30}$$

The potential difference between two electrodes separated by a displacement **R** *and equidistant from the current-dipole vector* **p** *measures the instantaneous projection of vector* **p** *on* **R**.

If the depolarization can be described by a single current-dipole vector, only three measurements are needed in principle, corresponding to the projections on three perpendicular axes. The standard electrocardiogram (ECG) records 12 potential differences using nine electrodes. There are many reasons for this. The body is not an infinite, homogeneous conductor, and the relationship between cellular dipole moments and the potential is more complicated than our model; to convert the three perpendicular components to the instantaneous values of **p** would require a mathematical reconstruction; and the electrodes are not far away compared to the size of the heart. With 12 recorded potential differences, it is fairly easy to interpret the electrocardiogram by inspection.

The first three electrodes are placed on each wrist and the left leg. The limbs serve as extensions of the wires, so that the potential is measured where the limbs join the body. This is a major correction to our crude model that the heart is in an infinite conducting medium. If the subject were immersed in a conducting medium such as sea water, movement of the arms would change the size of the ECG signal because it would change **R**. In air, however, movement of the arms does not change the size of the signal. The simplest correction to explain this is to say that **R** for the two arm electrodes goes from shoulder to shoulder. These three electrodes measure potential differences between three points located approximately as shown in Fig. 7.19. The dimensions are for a typical adult. The three potential differences are called *limb leads* I, II, and III:

$$\begin{aligned} \mathrm{I} &= v_B - v_A, \\ \mathrm{II} &= v_C - v_A, \\ \mathrm{III} &= v_C - v_B. \end{aligned} \tag{7.31}$$

In the approximation used here, the voltage difference I is proportional to the projection of **p** on $\mathbf{R}_\mathrm{I}$, and so forth. These leads measure the projections of **p** on the three vectors $\mathbf{R}_\mathrm{I}$, $\mathbf{R}_\mathrm{II}$, and $\mathbf{R}_\mathrm{III}$ of Fig. 7.19.

It is customary also to combine these three potentials in a slightly different way to obtain projections of **p** on three other directions. These combinations are called the *augmented limb leads*. They contain no information that was not already present in the limb leads, but the six signals are easier to interpret by inspection. The combinations are

$$aVR = v_A - \frac{1}{2}(v_B + v_C) = -\frac{1}{2}(\mathrm{I} + \mathrm{II}),$$

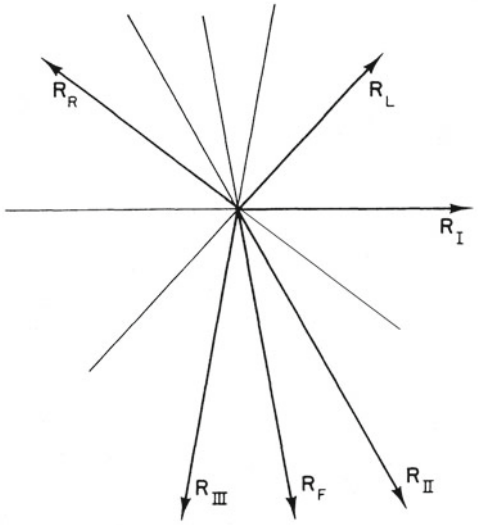

Fig. 7.20 The six directions in the frontal plane defined by the limb leads and the augmented limb leads. The angles are for the same subject as in Fig. 7.19

$$aVL = v_B - \frac{1}{2}(v_A + v_C) = \frac{1}{2}(\text{I} - \text{III}), \text{ and} \qquad (7.32)$$
$$aVF = v_C - \frac{1}{2}(v_A + v_B) = \frac{1}{2}(\text{II} + \text{III}).$$

These are proportional to the projections of $\mathbf{p}$ on vectors $\mathbf{R}_L$, $\mathbf{R}_R$, and $\mathbf{R}_F$ of Fig. 7.20. The subscripts refer to the fact that the vectors point toward the left shoulder, right shoulder, and foot, respectively.

The six lines in Fig. 7.20 are spaced approximately every 30° in the frontal plane. Many texts argue that the leads are spaced exactly every 30° and that the triangle of Fig. 7.19 is an equilateral triangle (Einthoven's triangle). While the directions are not far from 30°, this assumption is not really necessary. Physicians often want to know the direction of $\mathbf{p}$ at some point during the cardiac cycle, or the average direction of $\mathbf{p}$ during the QRS wave (ventricular depolarization). With six directions measured, this can be determined by inspection.

These six leads measure projections in the frontal plane. It is also necessary to have at least one projection in a plane perpendicular to the frontal plane. It is customary to place six leads across the chest wall in front of the heart; they are called the *precordial leads*. Their locations are shown in Fig. 7.21. The potential difference is measured between each precordial electrode and the average of v_A, v_B, and v_C. A lead therefore measures the projection of $\mathbf{p}$ on a vector from the center of triangle ABC to the electrode for that lead. This fact is not obvious, and in fact is true only if differences in $1/r^2$ are neglected. To see that it is true with the appropriate approximation, pick an arbitrary point O and from it construct vectors $\mathbf{R}_A$, $\mathbf{R}_B$, $\mathbf{R}_C$, and $\mathbf{R}_D$ to the points A, B, and C

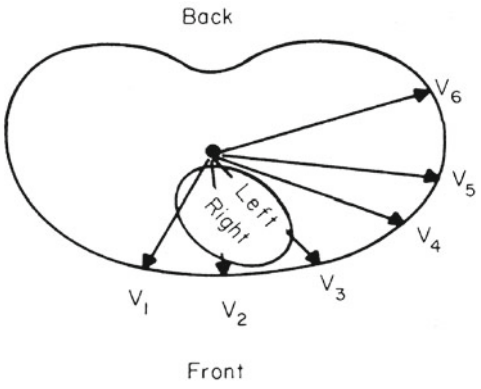

Fig. 7.21 The location of the precordial leads and the directions of the components of $\mathbf{p}$ which they measure. Reprinted with permission from Hobbie 1973. Copyright 1973, American Association of Physics Teachers

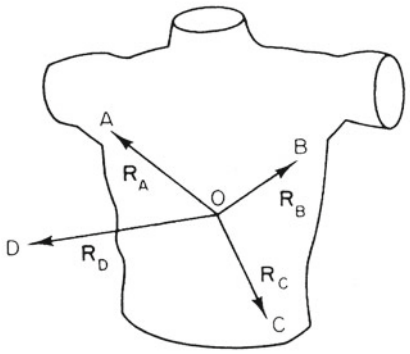

Fig. 7.22 A perspective drawing of the vectors used to calculate the potential in a precordial lead. Reprinted with permission from Hobbie 1973. Copyright 1973, American Association of Physics Teachers

of Fig. 7.22 and to the precordial electrode at D. The desired potential is

$$v = v_D - \frac{v_A + v_B + v_C}{3}.$$

It can be calculated using Eq. 7.30 for each term:

$$v = \frac{1}{4\pi\sigma_o}\left[\frac{\mathbf{p}\cdot\mathbf{R}_D}{R_D^3} - \frac{1}{3}\left(\frac{\mathbf{p}\cdot\mathbf{R}_A}{R_A^3} + \frac{\mathbf{p}\cdot\mathbf{R}_B}{R_B^3} + \frac{\mathbf{p}\cdot\mathbf{R}_C}{R_C^3}\right)\right].$$

So far, the location of O is arbitrary. If it is picked to be at the center of the triangle, then $\mathbf{R}_A + \mathbf{R}_B + \mathbf{R}_C = 0$. (This is the definition of center.) Since $R_A \approx R_B \approx R_C$, the term in large parentheses vanishes. The desired potential difference is then

$$v = \frac{1}{4\pi\sigma_o}\frac{\mathbf{p}\cdot\mathbf{R}_D}{R_D^3}.$$

In this approximation, each precordial lead measures the projection of $\mathbf{p}$ on a vector from the center of the triangle ABC to the electrode. The amplitude of the signal will be larger

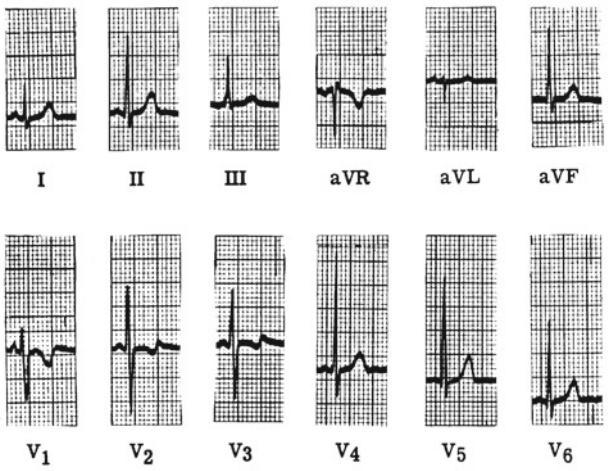

Fig. 7.23 A normal electrocardiogram. The large divisions are 0.5 mV vertically and 0.2 s horizontally. Reprinted with permission from Hobbie 1973. Copyright 1973, American Association of Physics Teachers. The electrocardiogram was supplied by Prof. James H. Moller, MD

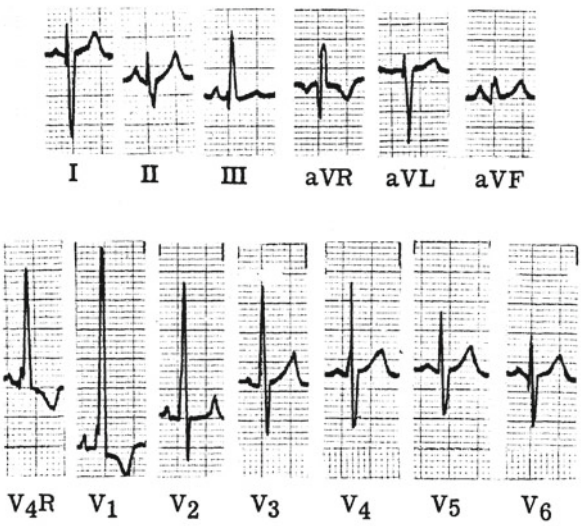

Fig. 7.24 The electrocardiogram of a patient with right ventricular hypertrophy. Reprinted with permission from Hobbie 1973. Copyright 1973, American Association of Physics Teachers. The electrocardiogram was supplied by Prof. James H. Moller, MD

than for the limb leads, because $R_D < R_A$. Some of the precordial leads are quite close to the heart. The assumption that r is the same for all parts of the myocardium is not valid. Because of the factor $1/r^2$, the greatest contribution to the potential comes from the closest regions of myocardium. A lead is said to "look at" the myocardium closest to it.

7.8 Some Electrocardiograms

A normal electrocardiogram is shown in Fig. 7.23. When **p** has its greatest magnitude during the QRS wave, it is nearly parallel to $\mathbf{R}_{\text{II}}$. There is almost no signal in aVL, which is perpendicular to $\mathbf{R}_{\text{II}}$.

Compare this to Fig. 7.24, which shows the electrocardiogram for a patient with *right ventricular hypertrophy*, an enlargement and thickening of the right ventricle. Because of the greater right ventricular muscle volume, **p** points to the right during the QRS wave, so that the QRS signal is negative in lead I. Lead aVF shows that there is very little vertical component of **p** during the QRS wave. The precordial leads V_1 and V_2 show the strongest signals, because the right ventricle faces the front of the body. In this case an extra lead V_4R has been used, which is symmetrical with V_4 but on the right side of the body.

The electrocardiogram in Fig. 7.25 is from a patient with left ventricular hypertrophy. The thicker left ventricular wall causes the QRS dipole to point to the left. As a result, lead I has an abnormally high peak, aVL is large and positive,

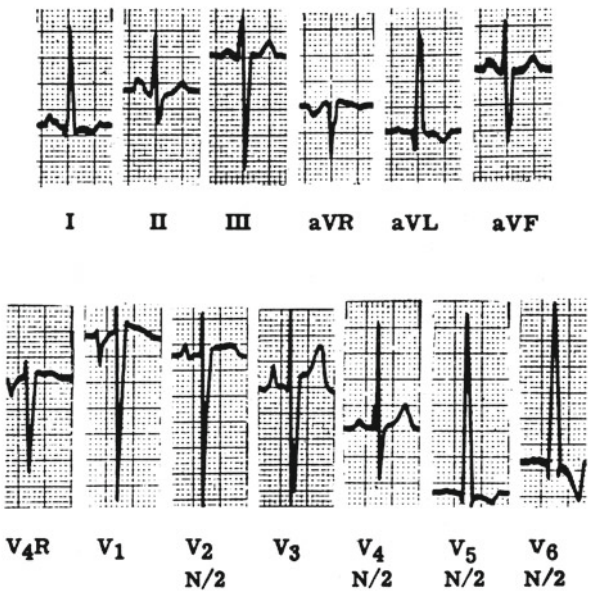

Fig. 7.25 The electrocardiogram for a patient with left ventricular hypertrophy. Reprinted with permission from Hobbie 1973. Copyright 1973, American Association of Physics Teachers. The electrocardiogram was supplied by Prof. James H. Moller, MD

V_2 is negative, and V_4, V_5, and V_6 have very large positive peaks. These last four leads are shown at half scale.

A fault in the conduction system known as a *bundle branch block* causes the depolarization wave to travel

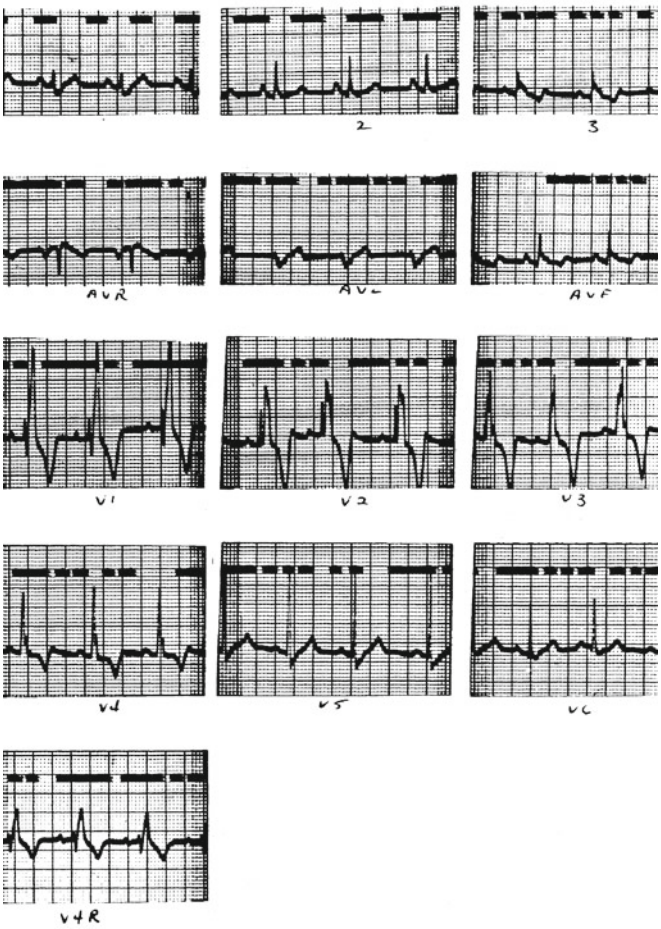

Fig. 7.26 The electrocardiogram for a patient with right bundle branch block. The electrocardiogram was supplied by Prof. James H. Moller, MD

through the myocardium rather than over the conduction system. Since the speed of propagation in myocardium is slower than that in the conduction system, the depolarization takes longer than usual. An electrocardiogram for a patient with *right bundle branch block* (a block in the bundle for the right ventricle) is shown in Fig. 7.26. The effect is most striking in leads that are most sensitive to the right ventricle: precordial leads 1 and 2. In V_1 the early part of the QRS wave has the usual biphasic, up–down pattern as the left ventricle depolarizes. This is followed by a large and prolonged vector pointing to the right, as the right ventricle slowly depolarizes. Lead V_2 shows a strong and prolonged bipolar signal as the right ventricle depolarizes.

7.9 Refinements to the Model

Our model for the potential outside a nerve or muscle cell has been a long single conducting fiber in an infinite, homogeneous medium. We will consider four ways to extend and improve the model. The first is to recognize that current must also flow radially inside the cell. If it did not, it could never leave the cell. At the same time we will abandon the assumption that the presence of the cell along the x axis does not perturb the current outside the cell. The third improvement is to recognize that the conductivity may depend on position. This is particularly important outside the cell, where there are muscle, fat, lungs, etc. Finally, the conductivity at a given point may depend on which direction the current flows–for example, parallel or perpendicular to the cells.

In order to make these refinements to the model, we must develop a different formulation of the problem. Consider some region of space containing a conducting material described by Ohm's law. The electric field is related to the potential by Eq. 6.16b: $\mathbf{E} = -\text{grad}\, v = -\nabla v$. If the material is isotropic and obeys Ohm's law, then from Eq. 6.26

$$\mathbf{j} = \sigma \mathbf{E} = -\sigma \nabla v. \tag{7.33}$$

We now apply the equation of continuity or conservation of charge, casting Eq. 4.8 in terms of the electric current density $\mathbf{j}$ and the electric charge per unit volume, ρ:

$$\frac{\partial \rho}{\partial t} = -\nabla \cdot \mathbf{j}. \tag{7.34}$$

Combining these two equations gives

$$\frac{\partial \rho}{\partial t} = \text{div}(\sigma \text{ grad } v) = \nabla \cdot (\sigma \nabla v). \tag{7.35}$$

Leaving the conductivity inside the divergence term allows the conductivity to depend on position. If the conductivity is the same everywhere it can be taken outside the divergence operator to give

$$\frac{\partial \rho}{\partial t} = \sigma \nabla^2 v = \sigma \left(\frac{\partial^2 v}{\partial x^2} + \frac{\partial^2 v}{\partial y^2} + \frac{\partial^2 v}{\partial z^2} \right). \tag{7.36a}$$

We can write this in cylindrical coordinates, which are more useful for modeling a cylindrical cell stretched along the z axis. From Appendix L, assuming that the potential does not depend on the angle ϕ, we have

$$\frac{\partial \rho}{\partial t} = \sigma \nabla^2 v = \sigma \left[\frac{1}{r} \frac{\partial}{\partial r} \left(r \frac{\partial v}{\partial r} \right) + \frac{\partial^2 v}{\partial z^2} \right]. \tag{7.36b}$$

These are very general equations, applicable to any volume of space where the material is homogeneous and isotropic and obeys Ohm's law. They were derived using Ohm's law and the conservation of charge. Equation 7.36a is actually the same result we had in Eq. 6.51. This is demonstrated in Problem 29.

7.9.1 The Fiber Has a Finite Radius

Now we can make the first two improvements: we relax the assumption that the fiber radius is very small. Except at the cell membrane, where charge on the membrane capacitance is changing as the membrane potential changes, $\partial\rho/\partial t = 0$. If we assume that the transmembrane potential v_m is known, then Eq. 7.36b can be applied separately to the extracellular and the intracellular fluid for a long straight fiber to determine the potential everywhere outside (or inside). This was first done by Clark and Plonsey (1968). In the extracellular and intracellular fluids, Eq. 7.36b becomes

$$\begin{aligned} \frac{1}{r}\frac{\partial}{\partial r}\left(r\frac{\partial v_o(r,z)}{\partial r}\right)+\frac{\partial^2 v_o(r,z)}{\partial z^2}=0, \quad r>a \\ \frac{1}{r}\frac{\partial}{\partial r}\left(r\frac{\partial v_i(r,z)}{\partial r}\right)+\frac{\partial^2 v_i(r,z)}{\partial z^2}=0, \quad r<a \\ v_m(z)=v_i(a,z)-v_o(a,z). \end{aligned} \tag{7.37}$$

With v_m known, these equations were solved for the potential distribution inside and outside the cell. This is the calculation that was done to obtain Fig. 7.13. The result of this type of calculation has been compared to the line-source model by Trayanova et al. (1990).

7.9.2 Nonuniform Exterior Conductivity

To make the next improvement, consider an extracellular region in which the conductivity is not uniform. In a region without sources, the potential obeys

$$\nabla\cdot(\sigma_o\nabla v_o)=0. \tag{7.38}$$

Often, the conductivity is assumed to be "piecewise" homogenous, with a different value assigned to each kind of tissue. Within each tissue the potential then obeys Laplace's equation, $\nabla^2 v_o = 0$. At the boundary between tissues, the potential and the normal component of the current are continuous.

When the different tissues have realistic and irregular boundaries, special techniques are needed to solve Laplace's equation. One important technique is the *finite-element method* (Miller and Henriquez 1990); another is the *boundary-element method* (Gulrajani 1998).

A typical application, which serves as the basis for *noninvasive electrocardiographic imaging*, is to measure the potential at the body surface and then calculate the potential on the epicardium (the outer surface of the heart; Rudy and Burnes 1999; Stanley et al. 1986). One cannot calculate the potential inside the heart unless the sources are known, but finding the potential on the epicardial surface is possible.

7.9.3 Anisotropic Conductivity: The Bidomain Model

The final improvement recognizes that the cardiac tissue is generally not isotropic. If it is still described by Ohm's law, then we can write $\mathbf{j}=\widetilde{\sigma}\cdot\mathbf{E}$ where $\widetilde{\sigma}$ is a matrix or tensor. In Cartesian coordinates

$$\begin{pmatrix} j_x \\ j_y \\ j_z \end{pmatrix} = \begin{pmatrix} \sigma_{xx} & \sigma_{xy} & \sigma_{xz} \\ \sigma_{yx} & \sigma_{yy} & \sigma_{yz} \\ \sigma_{zx} & \sigma_{zy} & \sigma_{zz} \end{pmatrix} \begin{pmatrix} E_x \\ E_y \\ E_z \end{pmatrix}. \tag{7.39}$$

This is a compact notation for

$$j_x=\sigma_{xx}E_x+\sigma_{xy}E_y+\sigma_{xz}E_z,$$

with similar equations for j_y and j_z. It can be shown that the conductivity matrix must be symmetric, so there are actually six conductivity coefficients, not nine. It is often possible to make some of the matrix elements zero by suitable choice of a coordinate system and suitable orientation of the axes.

Problem 29 shows that for a small cylindrical region of isotropic axoplasm of length h and radius a, the cylindrical surface of which is surrounded by cell membrane, the total charge Q within the axoplasm changes according to

$$\frac{\partial Q}{\partial t}=\pi a^2 h\frac{\partial\rho_i}{\partial t}=C\frac{\partial v_m}{\partial t}+i_m=2\pi a h\left(c_m\frac{\partial v_m}{\partial t}+j_m\right),$$

or

$$c_m\frac{\partial v_m}{\partial t}+j_m=\frac{\pi a^2 h}{2\pi a h}\sigma_i\frac{\partial^2 v_i}{\partial x^2}=\frac{\sigma_i a}{2}\frac{\partial^2 v_i}{\partial x^2}.$$

This can also be written as

$$\beta\left(c_m\frac{\partial v_m}{\partial t}+j_m\right)=\sigma_i\frac{\partial^2 v_i}{\partial x^2},$$

where $\beta = 2\pi a h/\pi a^2 h = 2/a$ is the ratio of surface area to volume of the cell. Our cell was cylindrical. With other geometrical configurations, such as a cubic or a spherical cell, β would have a different value, but it always has the dimensions of $(\text{length})^{-1}$. In the general three-dimensional anisotropic case, the equivalent equation is

$$\underbrace{\beta\left(c_m\frac{\partial v_m}{\partial t}+j_m\right)}_{\text{zero, except at the cell membrane}} = \operatorname{div}(\widetilde{\sigma}_i\ \operatorname{grad} v_i)=\nabla\cdot(\widetilde{\sigma}_i\nabla v_i). \tag{7.40}$$

Both σ_i and v_i are functions of position. The left-hand side is zero except at the cell membrane. The main theme of this chapter has been that current that stops flowing inside the cell must flow outside the cell. We can write an analogous equation for the region outside the cell:

$$\underbrace{-\beta\left(c_m\frac{\partial v_m}{\partial t}+j_m\right)}_{\text{zero, except at the cell membrane}} = \nabla\cdot(\widetilde{\sigma}_o\nabla v_o). \tag{7.41}$$

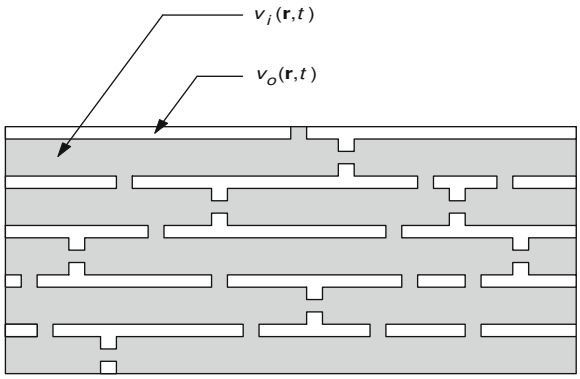

Fig. 7.27 The interior of myocardial cells (*shaded*) is connected to adjoining cells by gap junctions. The bidomain model assumes that in a small region of space (large compared to a cell) there are two potentials: the interior potential and outside potential that are functions of position and time

Myocardial cells are typically about 10 μm in diameter and 100 μm long. They have the added complication that they are connected to one another by gap junctions, as shown schematically in Fig. 7.27. This allows currents to flow directly from one cell to another without flowing in the extracellular medium. The *bidomain* (two-domain) model is often used to model this situation (Henriquez 1993; Henriquez and Ying 2009). It considers a region, small compared to the size of the heart, that contains many cells and their surrounding extracellular fluid. It simplifies the problem by assuming that each small volume element contains two domains, intracellular and extracellular. Think of the volume element as the entire region shown in Fig. 7.27. There are two potentials in each small volume element: $v_i(\mathbf{r},t)$ and $v_o(\mathbf{r},t)$. These potentials are averages over the intracellular and extracellular domains contained in the volume element. The transmembrane potential is the difference between these two potentials: $v_m(\mathbf{r},t) = v_i(\mathbf{r},t) - v_o(\mathbf{r},t)$. Charge can pass between the two domains, but the total charge within a volume element is conserved. If the current densities in each domain are $\mathbf{j}_i$ and $\mathbf{j}_o$, then the divergence of the sum is zero: $\nabla\cdot(\mathbf{j}_i+\mathbf{j}_o)=0$. The divergence of each current individually passes through the membrane or charges the membrane capacitance. The anisotropic analogs of Eqs. 7.40 and 7.41 are now

$$\begin{aligned}\beta\left(c_m\frac{\partial v_m}{\partial t}+j_m\right) &= \operatorname{div}(\widetilde{\sigma}_i\cdot\operatorname{grad}v_i)=\nabla\cdot(\widetilde{\sigma}_i\cdot\nabla v_i),\\ -\beta\left(c_m\frac{\partial v_m}{\partial t}+j_m\right) &= \operatorname{div}(\widetilde{\sigma}_o\cdot\operatorname{grad}v_o)\\ &= \nabla\cdot(\widetilde{\sigma}_o\cdot\nabla v_o).\end{aligned} \tag{7.42}$$

The quantity β is the membrane surface area per unit volume of the entire bidomain—both intracellular and extracellular volumes. For example, if we consider that the cells are all cylindrical of length h and radius a, then the surface area of a cell is $2\pi ah$. If the fraction of the total volume occupied by cells is f, then the total volume associated with this cell is $\pi a^2 h/f$, so

$$\beta=\frac{2f}{a}. \tag{7.43}$$

The membrane current j_m can be modeled by either a passive membrane (Ohm's law—electrotonus) or with one of the models for an active membrane.

Anisotropy plays an important role in the bidomain model. To see why, consider a solution to Laplace's equation in a monodomain—a two-dimensional sheet of homogeneous, anisotropic tissue with straight fibers. If the x direction is chosen to be along the fiber direction (the direction of greatest conductivity), then Laplace's equation becomes

$$\sigma_{ox}\frac{\partial^2 v_o}{\partial x^2}+\sigma_{oy}\frac{\partial^2 v_o}{\partial y^2}=0.$$

Now define a new set of coordinates $x'=x$ and $y'=\sqrt{\sigma_{ox}/\sigma_{oy}}\,y$. You can show that in these new coordinates Laplace's equation becomes

$$\frac{\partial^2 v_o}{\partial x'^2}+\frac{\partial^2 v_o}{\partial y'^2}=0.$$

We have removed the effect of anisotropy by rescaling distance in the direction perpendicular to the fibers. If you try a similar trick with the bidomain model

$$\sigma_{ix}\frac{\partial^2 v_i}{\partial x^2}+\sigma_{iy}\frac{\partial^2 v_i}{\partial y^2}=\beta\left(c_m\frac{\partial v_m}{\partial t}+j_m\right) \tag{7.44a}$$

$$\sigma_{ox}\frac{\partial^2 v_o}{\partial x^2}+\sigma_{oy}\frac{\partial^2 v_o}{\partial y^2}=-\beta\left(c_m\frac{\partial v_m}{\partial t}+j_m\right), \tag{7.44b}$$

you can find a new coordinate system that removes the effect of anisotropy in either the intracellular space or the extracellular space, but in general you cannot find a coordinate system that removes the anisotropy in both spaces simultaneously (Roth 1992). Only in the special case of equal anisotropy ratios ($\sigma_{ix}/\sigma_{iy}=\sigma_{ox}/\sigma_{oy}$) will the equations simplify dramatically. But the anisotropy ratios in the heart are not equal. In the intracellular space the ratio of conductivities parallel and perpendicular to the fibers is about 10:1, while in the extracellular space this ratio is about 4:1 (Roth 1997). Anisotropy plays an essential role in the electrical behavior of the heart, especially during electrical stimulation.

7.10 Electrical Stimulation

The information that has been developed in this chapter can also be used to understand some of the features of stimulating electrodes. These may be used for electromyographic

studies; for stimulating muscles to contract called *functional electrical stimulation* (Peckham and Knutson 2005); for a *cochlear implant* to partially restore hearing (Zeng et al. 2008); deep brain stimulation for Parkinson's disease (Perlmutter and Mink 2006); for cardiac pacing (Moses and Mullin 2007); and even for defibrillation (Dosdall et al. 2009). The electrodes may be inserted in cells, placed in or on a muscle, or placed on the skin.

A pulse of current is sent to the stimulating electrode. The current required to produce a response depends on the shape and size of the electrode, its placement, the kind of cell being stimulated, and the duration of the pulse. For a given electrode geometry the shorter the pulse, the larger the current required for a tissue response. For very long pulses there is a minimum current required to stimulate that is called *rheobase*. The *strength-duration curve* was first discovered by Weiss in 1901. He expressed it in terms of total charge in the stimulating pulse. A description of the strength-duration curve and its history has been given by Geddes and Bourland (1985). They also describe some techniques for making accurate measurements. The strength-duration curve for current was first described by Lapicque (1909) as

$$i = i_R \left(1 + \frac{t_C}{t}\right), \tag{7.45}$$

where i is the current required for stimulation, i_R is the rheobase, t is the duration of the pulse, and t_C is chronaxie, the duration of the pulse that requires twice the rheobase current.

Equation 7.45 provides an empirical fit to the experimental data. We can develop a model to explain it using information from Chap. 6. A nerve fires after a certain departure from the resting potential. Subthreshold behavior can be modeled by electrotonus. Suppose that we inject a stimulating current into a cell at the origin. Equation 6.58 gave the voltage along the axon for a current injected in the cell at the origin after an infinitely long time: $v - v_r = v_0 e^{-|x|/\lambda}$. The solution to Problem 6.34 shows that the current injected is

$$i_0 = 2v_0/\lambda r_i. \tag{7.46}$$

The quantities λ and r_i are defined in Chap. 6. The factor of 2 arises because current flows both ways along the cell. The rheobase current is

$$i_R = 2\frac{v_{\text{threshold}}}{\lambda r_i}. \tag{7.47}$$

If we assume that the threshold voltage is independent of pulse duration, we can use the curve for $x = 0$ in Fig. 6.31c to relate the minimum current to the pulse duration. As long as the pulse is applied, the voltage will rise along this curve. When the current is turned off, the voltage will start to fall. If the voltage reaches threshold, the cell will fire. This

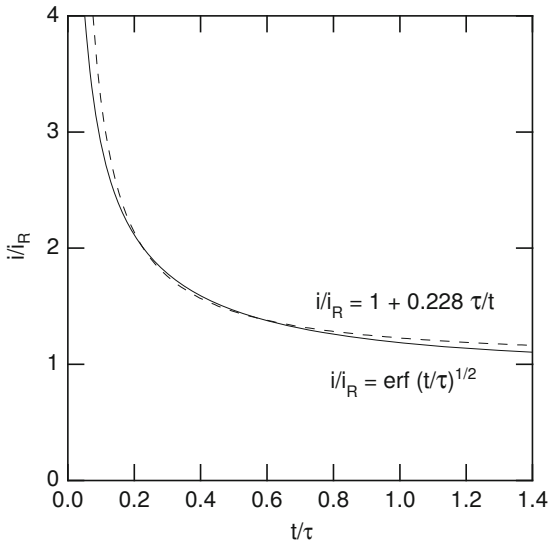

Fig. 7.28 The stimulus strength-duration curve plotted for the chronaxie–rheobase model, Eq. 7.45 and for electrotonus, Eq. 7.49

curve is the solution of Eq. 6.55. The solution is (Chap. 6, Problem 36; Plonsey 1969, p. 132))

$$v(0,t) - v_r = v_0 \operatorname{erf}\left(\sqrt{\frac{t}{\tau}}\right), \tag{7.48}$$

where τ is the membrane time constant, $\kappa\epsilon_0\rho_m$. The error function is defined in Eq. 4.74 and is plotted in Fig. 4.21. The current required for stimulation with an intracellular electrode at the origin is therefore

$$i = \frac{2v_{\text{threshold}}}{\lambda r_i \operatorname{erf}(\sqrt{t/\tau})} = \frac{i_R}{\operatorname{erf}(\sqrt{t/\tau})}. \tag{7.49}$$

Chronaxie can be related to the time constant τ by setting $i = 2i_R$:

$$2i_R = \frac{i_R}{\operatorname{erf}\left(\sqrt{t_C/\tau}\right)}. \tag{7.50}$$

From a table of values of the error function, we find

$$t_C = 0.228\tau. \tag{7.51}$$

Figure 7.28 compares the standard empirical curve, Eq. 7.45, with this model. The curves are experimentally indistinguishable.

Equation 7.45 is also used for surface electrodes. Table 7.1 shows some experimental values for rheobase and chronaxie. The further the electrode from the tissue being stimulated, the greater the rheobase current that is required.

An electrode that is transferring positive charge to the medium is called an *anode*. One that is collecting positive charge is called a *cathode*. If the stimulating electrode is

Table 7.1 Comparison of values for rheobase and chronaxie for different stimulations

Stimulation	Rheobase (mA)	Chronaxie (ms)
Intracellular, from Table 6.1, $v_{\text{threshold}} = 15\,\text{mV}$	6.7×10^{-6}	0.23
Myocardium, from good pacing electrodes	0.1	
Motor nerves for inspiration, from stimulation of chest wall (Voorhees et al. 1992)	49	0.17
Myocardium, from stimulation of chest wall (Voorhees et al. 1992)	204	1.82

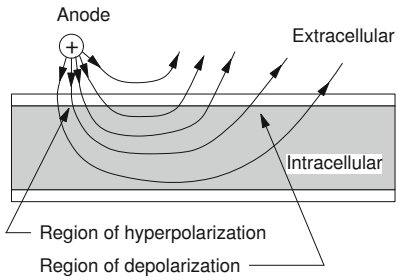

Fig. 7.29 A schematic drawing showing why there is a region of hyperpolarization near a stimulating anode (positive electrode) with a region of weaker depolarization further away

inside the cell, a positive current leaving the electrode will increase the positive charge within the cell and depolarize it. Another way to say it is that current from the electrode flows out through the membrane, so the inside of the membrane will be made more positive than the outside. On the other hand, an anodic electrode just outside the cell will send positive current in through the membrane near the electrode, as shown in Fig. 7.29. This lowers the potential inside and hyperpolarizes the membrane near the electrode. Further away from the stimulation point will be a region where current flows out through the membrane, thus depolarizing the cell. However, the outward current is in general spread out over more membrane, so the current density and hence the depolarization is less than the hyperpolarization near the anode. The situation is, of course, reversed for a cathodic electrode. Figure 7.29 is conceptual; to draw the field lines accurately would require taking into account the conductivities of the extracellular and intracellular fluid as well as the membrane.

The electrotonus model also helps us understand another effect that is observed: the *virtual cathode*. The point of origin for a stimulus can be measured by placing sensing electrodes in or on the heart at different distances from the stimulating electrode and plotting the time required for the depolarization wave front to reach the electrode vs. its position. Extrapolation to the time of stimulus gives the size of the region of initial depolarization. Imagine a stimulating electrode inside a one-dimensional cell. When the stimulus current is just above rheobase, the region of depolarization is very small and surrounds the electrode. As the stimulating current is increased, the size of the initial depolarized region grows. From Eqs. 6.58 and 7.50 we obtain

$$v_{\text{threshold}} = \frac{i_0 \lambda r_i}{2} e^{-x_{\text{vc}}/\lambda}$$

or

$$x_{\text{vc}} = \lambda \ln\left(\frac{i_0 \lambda r_i}{2 v_{\text{threshold}}}\right) = \lambda \ln\left(\frac{i_0}{i_R}\right), \tag{7.52}$$

where x_{vc} is the size of the virtual cathode.

Cardiac pacemakers are a useful treatment for certain heart diseases (Jeffrey 2001; Moses and Mullin 2007; Barold 1985). The most frequent are an abnormally slow pulse rate (*bradycardia*) associated with symptoms such as dizziness, fainting (*syncope*), or heart failure. These may arise from a problem with the SA node (*sick sinus syndrome*) or with the conduction system (*heart block*). One of the first uses of pacemakers was to treat complete or *third degree* heart block. The SA node and the atria fire at a normal rate but the wave front cannot pass through the conduction system. The AV node or some other part of the conduction system then begins firing and driving the ventricles at its own, pathologically slower rate. Such behavior is evident in the ECG in Fig. 7.30, in which the timing of the QRS complex from the ventricles is unrelated to the P wave from the atria. A pacemaker stimulating the ventricles can be used to restore a normal ventricular rate.

A pacemaker can be used temporarily or permanently. The pacing electrode can be threaded through a vein from the shoulder to the right ventricle (*transvenous pacing*, Fig. 7.31) or placed directly in the myocardium during heart surgery. Sometimes two pacing electrodes are used, one in the atrium and one in the ventricle. The pacing electrode can be unipolar or bipolar. With a unipolar electrode, the stimulation current flows into the myocardium and returns to the case of the pacemaker, which is often placed in a pocket in the muscle of the chest wall near the shoulder. The return current in a bipolar electrode goes to a ring electrode a few centimeters back along the pacing lead from the electrode at the tip. The surface area of a typical tip is about 10 mm^2 ($10^{-5}\,\text{m}^2$). The current density required to initiate depolarization depends on the spatial distribution of the current and is approximately 100 A m^{-2}. Thus, in this model the current is about 1 mA.[6] The resistance of the tissue is typically 500 Ω, so the voltage is 0.5 V. After the pacing electrode is implanted, the size of the voltage pulse required to initiate ventricular activity rises because inflammatory tissue grows around the electrode. It is conducting, but the myocardium is further away, and the

[6] Acute implants of smaller electrodes where the electrode resistance is low, as well as computer simulations, have shown stimulation with currents as small as 18 μA (Lindemans and Denier van der Gon 1978).

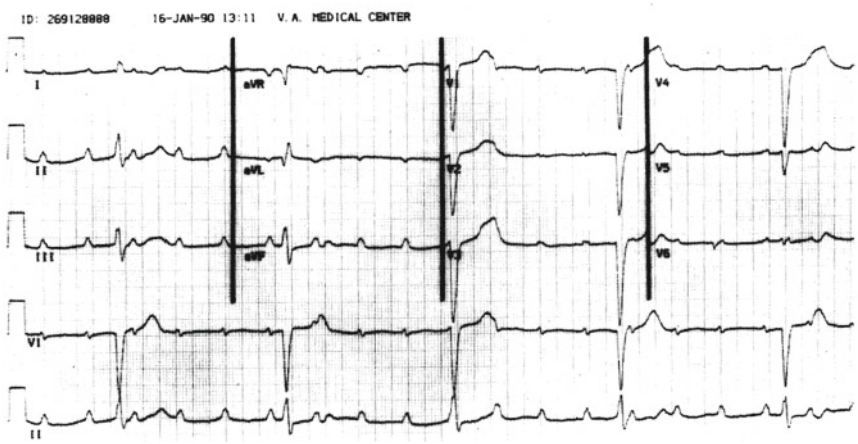

Fig. 7.30 A patient with 3rd degree AV heart block. (From Rardon et al. 2000. Used by permission)

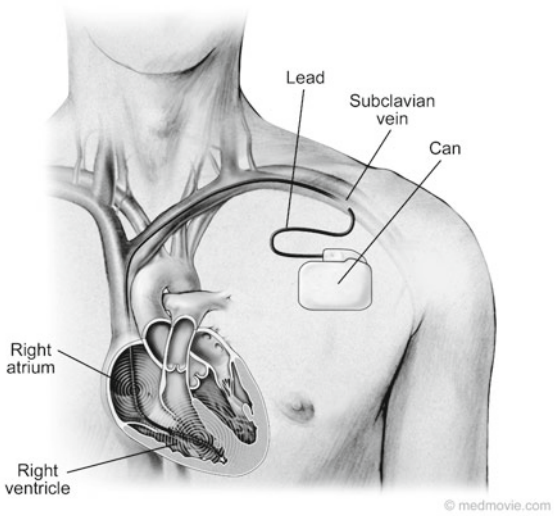

Fig. 7.31 An implanted pacemaker or defibrillator. The battery and electronics are in a sealed container (the "can") placed under the skin near the left shoulder. The electrode or "lead" is threaded through the subclavian vein and right atrium into the right ventricle. (Image © Copyright by medmovie.com. Used by permission of medmovie.com)

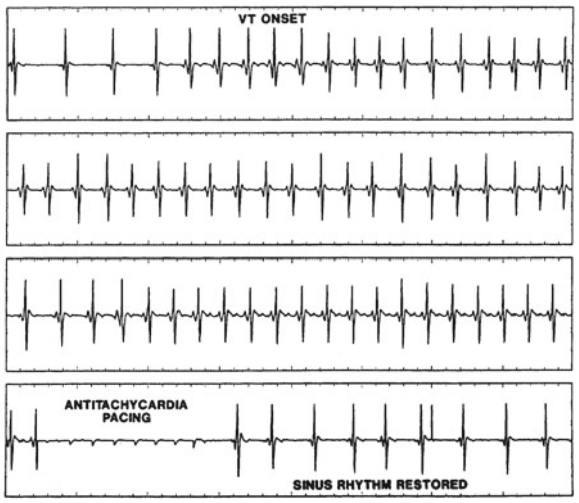

Fig. 7.32 The top strip shows the onset of ventricular tachycardia, which persists in the next two strips. Very rapid pacing in the fourth strip restores a normal sinus rhythm. (Source: Mitrani et al. 1995. Used by permission)

inflammatory tissue effectively increases the size of the electrode, thereby reducing the current density. After 6 months or so, the inflammation has been replaced by a small fibrous capsule, resulting in an effective electrode size larger than the bare electrode but smaller than the region of inflammation. Electrodes that elute steroids have been used to reduce the inflammation.

Pacemakers can also be designed to detect an abnormal rhythm and apply an electrical stimulus to reverse it. Fig. 7.32 shows a patient with ventricular tachycardia due to a reentrant circuit (p. 194, 290) which has been corrected by pacing very rapidly so that the refractory period prevents the propagation of the reentrant wave. *Ventricular fibrillation* occurs when the ventricles contain many interacting reentrant wavefronts that propagate chaotically. Fibrillation is discussed in greater detail in Chap. 10. During fibrillation the ventricles no longer contract properly, blood is no longer pumped through the body, and the patient dies in a few minutes. Implantable defibrillators are similar to pacemakers, but are slightly larger. An implanted defibrillator continually measures the ECG. When a signal indicating fibrillation is sensed, it delivers a much stronger shock that can eliminate the reentrant wavefronts and restore normal heart rhythm (Fig. 7.33).

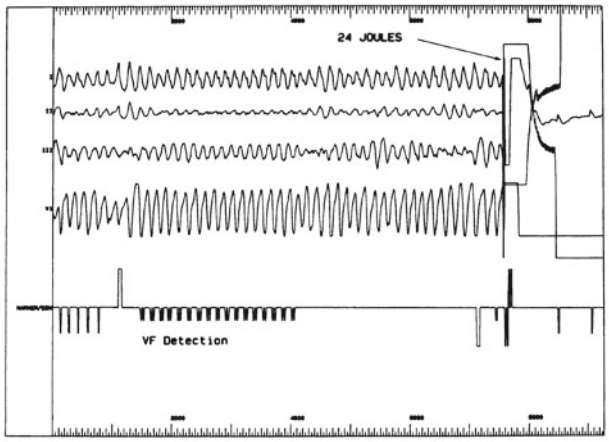

Fig. 7.33 Ventricular fibrillation has been induced in the electrophysiology laboratory. A pacemaker cardioverter-defibrillator detects the ventricular fibrillation. A capacitor is then charged and applies a 24-joule defibrillation pulse that restores normal rhythm. (Source: Mitrani et al. 1995)

The bidomain model has been used to understand the response of cardiac tissue to stimulation (Janks and Roth 2009; Trayanova and Plank 2009). This model explains a remarkable experimental observation. Although the speed of the wave front is greater along the fibers than perpendicular to them, if the stimulation is well above threshold, the wavefront originates farther from the cathode in the direction perpendicular to the fibers—the direction in which the speed of propagation is slower. The simulations show that this is due to the anisotropy in conductivity. This is called the *dog-bone* shape of the virtual cathode. It can rotate with depth in the myocardium because the myocardial fibers change orientation. The difference in anisotropy accentuates the effect of a region of hyperpolarization (a virtual anode) adjacent to the depolarization region produced by a cathodic electrode. This hyperpolarization can shorten the refractory period of the tissue, thereby creating new excitable paths through which reentrant wave fronts can propagate (Wikswo and Roth 2009; Ripplinger and Efimov 2009).

One of the fundamental problems with research in this area can be seen in equations like Eq. 7.41. The variable on the left is the transmembrane potential v_m. The variable on the right is the potential inside or outside the cell. Measurement of v_m requires measurement or calculation of the difference $v_i - v_o$. Experimental measurements of the transmembrane potential often rely on the use of a voltage-sensitive dye whose fluorescence changes with the transmembrane potential (*optical mapping*) (Rosenbaum and Jalife 2001).

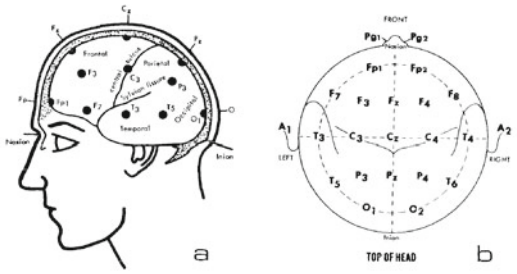

Fig. 7.34 The standard "10–20" arrangement of electrodes on the scalp for the EEG. (Courtesy of Natus Neurology Grass brand products)

7.11 The Electroencephalogram

Much can be learned about the brain by measuring the electric potential on the scalp surface. Such data are called the *electroencephalogram* (EEG). Nunez and Srinivasan (2005) have written an excellent book about the physics of the EEG. We briefly examine the topic here. The EEG is used to diagnose brain disorders, to localize the source of electrical activity in the brain in patients who have epilepsy (Lopes da Silva 2008), and as a research tool to learn more about how the brain responds to stimuli (*evoked responses*) and how it changes with time (*plasticity*). Typically, the EEG is measured from 21 electrodes attached to the scalp according to the *10–20 system* (Fig. 7.34). A typical signal from an electroencephalographic electrode is shown in the top panel of Fig. 11.39. One difficulty in interpreting the EEG is the lack of a suitable reference electrode. None of the 21 electrodes in Fig. 7.34 qualifies as a distant ground against which all other potential recordings can be measured. One way around this difficulty is to subtract from each measured potential the average of all the measured potentials. In the problems, you are asked to prove that this *average reference recording* does not depend on the choice of reference electrode; it is a reference-independent method.

Symbols Used in Chapter 7

Symbol	Use	Units	First used page
a	Axon radius	m	187
c_m	Membrane capacitance per unit area	F m^{-2}	200
f	Intracellular volume fraction		201
h	Length of segment	m	200
i	Current	A	186
i_i, i_o	Current inside, outside axon	A	186
i_R	Rheobase current	A	202
j, $\mathbf{j}$	Current density	A m^{-2}	186
j_m	Current density through membrane	A m^{-2}	200
p, $\mathbf{p}$	Activity vector or current dipole moment	A m	188
q	Charge	C	186
r_i	Resistance per unit length inside axon	Ω m^{-1}	202
r, $\mathbf{r}$	Distance	m	186
t	Time	s	199
t_C	Chronaxie	s	202
v	Potential	V	186
v_i, v_o	Potential inside, outside axon	V	200
v_m	Potential across membrane	V	200
x, y, z, x_0, x_1, x_2, y_0	Distance or position	m	187
x_{vc}	Size of virtual cathode	m	203
C	Capacitance	F	200
E, $\mathbf{E}$	Electric field	V m^{-1}	186
P_n	Legendre Polynomial		189
Q	Electric charge	C	200
R	Resistance	Ω	187
R, $\mathbf{R}$	Distance or position	m	190
β	Ratio of surface area to volume	m^{-1}	200
ϵ_0	Permittivity of free space	N^{-1} m^{-2} C^2	186
λ	Space constant	m	202
σ, σ_i, σ_o	Electrical conductivity	S m^{-1}	186
ρ	Charge density	C m^{-3}	199
τ	Time constant	s	202
θ	Angle		188
ξ	Ratio of x to R		192
Ω	Solid angle		189

Problems

Section 7.1

Problem 1. A single nerve or muscle cell is stretched along the x axis and embedded in an infinite homogeneous medium of conductivity σ_o. Current i_0 leaves the cell at $x = b$ and enters the cell again at $x = -b$. Find the current density $\mathbf{j}$ at distance r from the axis in the $x = 0$ plane.

Problem 2. An axon is stretched along the x axis. At one instant of time an impulse traveling along the axon has the form shown in the graph. The electrical conductivity inside the axon of radius a is σ_i. In the infinite external medium it is σ_o. Find an expression for the potential at point (x_0, y_0).

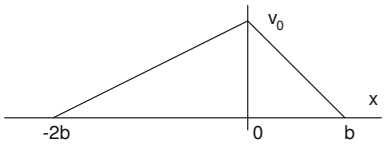

Problem 3. The interior potential of a cylindrical cell is plotted at one instant of time. Distances along the cell are given in terms of length b. The cell has radius a and electrical conductivity σ_i. The resting potential is 0 and the depolarized potential is v_0. The conductivity of the external medium is σ_o.

(a) Find expressions for, and plot, the current along the cell in the four regions $(x < 0, 0 < x < 2b, 2b < x < 3b, 3b < x)$.

(b) Find the potential at a point (x, y) outside the cell in terms of the parameters given in the problem. The point is not necessarily far from the cell.

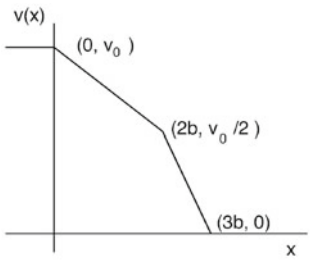

Section 7.2

Problem 4. Modify the closing argument of Sect. 7.2 by considering electrodes that are disks rather than spheres. (Hint: The capacitance you will need is given in Sect. 6.19.)

Problem 5. Suppose an axon is surrounded by a thin layer of extracellular fluid of thickness d. Use arguments based on the intracellular and extracellular resistances to estimate the ratio $\Delta v_o / \Delta v_i$ in this case.

Section 7.3

Problem 6. Starting with Eq. 7.4, make the Taylor's series expansions described in the text, and use them to derive Eq. 7.16.

Problem 7. What would be the current-dipole moment of a nerve cell of radius 2 μm when it depolarizes? Would myelination make any difference? Does the result depend on the rise time of the depolarization? If the impulse lasts 1 ms and the conduction speed is 5 m s^{-1}, how far apart are the rising and falling edges of the pulse?

Problem 8. An axon or muscle cell is stretched along the x axis on either side of the origin. As it depolarizes, a constant

current dipole **p** pointing to the right sweeps along the axis with velocity u. An electrode at $(x = 0, y = a)$ measures the potential with respect to $v = 0$ at infinity. Ignore repolarization. Find an expression for v at the electrode as a function of time and sketch it. Assume that at $t = 0$, **p** is directly under the electrode at $x = 0$.

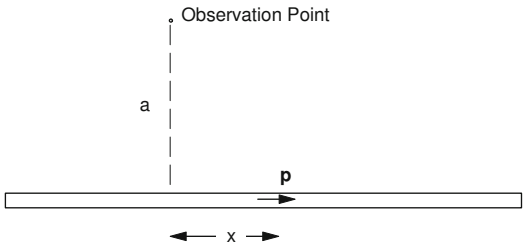

Problem 9. An electrode at $(x = 0, y = a)$ measures the potential outside an axon with respect to $v = 0$ at infinity. A nerve impulse is at point x along the axon, measured from the perpendicular from the electrode to the axon. At $x + b$ a current dipole points to the right, representing the depolarization wave front. At $x - b$ a vector of the same magnitude points to the left, representing repolarization. Obtain an expression for v as a function of x, b, p, and a. Plot it in the case $a = 1$, $b = 0.05$.

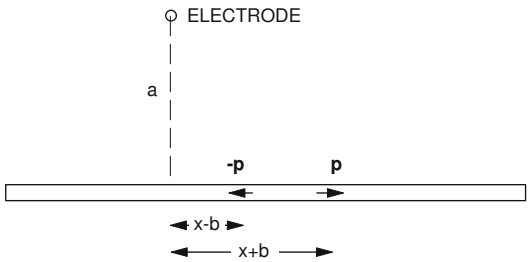

Problem 10. A dipole **p** located at the origin (0, 0, 0) is oriented in the x direction. The potential $v_o(x)$ produced by this dipole is measured along the line $y = 0$, $z = d$.

(a) Find an equation for $v_o(x)$ in terms of x, d, σ_o (the conductivity of the medium) and the dipole strength, p.

(b) Find an expression for the depth d of the dipole in terms of the distance Δx, defined as the distance between the minimum and maximum of $v_o(x, y)$. This is an example of an "inverse problem," in which you try to learn about the source (in this case, the depth of **p**) from measurements of v_o.

Problem 11. The *solid angle theorem* is often used to interpret electrocardiograms. The relationship between the exterior potential and the solid angle in Eq. 7.15 is a general result: the potential is proportional to the solid angle subtended by the wave front. Use this result to explain (a) why a closed wave front produces no exterior potential, and (b) why an open wave front produces a potential that depends only on the geometry of its opening or rim.

Section 7.4

Problem 12. Run the program of Fig. 7.11 and plot the potential for different distances from the axon.

Problem 13. Modify the program of Fig. 7.11 to calculate the potential from a single Gaussian action potential and plot the potential.

Problem 14. Let the intracellular potential be zero except in the range $-a < x < a$, where it is given by

$$v_i = \begin{cases} 2\left(\dfrac{a+x}{a}\right)^2, & -a < x < -a/2 \\ 1 - 2\left(\dfrac{x}{a}\right)^2, & -a/2 < x < a/2 \\ 2\left(\dfrac{a-x}{a}\right)^2, & a/2 < x < a. \end{cases}$$

Plot v_i vs x. Use Eq. 7.21 to calculate the exterior potential at (x_0, y_0). You may need the integral

$$\int \frac{dx}{\sqrt{x^2 + b^2}} = \sinh^{-1}\left(\frac{x}{b}\right).$$

Section 7.5

Problem 15. Suppose a wave front propagates at a speed of 0.25 m s^{-1} and its refractory period lasts 250 ms. Calculate the minimum path length of its reentrant circuit. Most reentrant wave fronts are somewhat slower and briefer than this, so their paths may be shorter.

Section 7.7

Problem 16. Two electrodes are placed in a uniform conducting medium 10 cm from a cell of radius 5 μm and 10 cm from each other, so that the two electrodes and the cell form an equilateral triangle. When the cell depolarizes the potential rises 90 mV. What will be the potential difference between the two electrodes when the cell orientation is optimum? How many cells would be needed to give a potential difference of 1 mV between the electrodes? Assume $\sigma_i/\sigma_o = 10$.

Problem 17. Guess whatever parameters you need to predict the voltage at the peak of the QRS wave in lead II. Compare your results to the electrocardiogram of Fig. 7.23.

Problem 18. At a particular instant of the cardiac cycle, **p** is located at the midpoint of a line connecting two electrodes that are 50 cm apart, and **p** is parallel to that line. At that instant the magnitude of the potential difference between the electrodes is 1.5 mV. Upon depolarization, the potential change within the cells has magnitude 90 mV.

(a) What is the magnitude of **p**?

(b) If $\sigma_i/\sigma_o = 10$, what is the cross-sectional area of the advancing region of depolarization?

Problem 19. A semi-infinite slab of myocardium occupies the region $z > 0$. A hemispherical wave of depolarization moves radially away from the origin through the slab. At some instant of time the radius of the hemispherical depolarizing wavefront is R. Assume that $\mathbf{p} = \int d\mathbf{p}$, that $d\mathbf{p}$ is everywhere perpendicular to the advancing wavefront, and that the magnitude of $d\mathbf{p}$ is proportional to the local area of the wavefront. Find $\mathbf{p}$. Assume that the observation point is very far away compared to R.

Problem 20. Make measurements on yourself and construct Fig. 7.19.

Problem 21. Experiments have been done in which a dog heart was stimulated by an electrode deep within the myocardium. No exterior potential difference was detected until the spherical wave of depolarization grew large enough so that part of it intercepted one wall of the heart. Why?

Problem 22. Prove directly from Eq. 7.32 that $\mathrm{I} - \mathrm{II} + \mathrm{III} = 0$. (It is sometimes said that the equilateral nature of Einthoven's triangle is necessary to prove this.)

Problem 23. Derive Eqs. 7.32.

Section 7.8

Problem 24. Estimate the lower limit for the duration of the QRS complex by calculating the time required for a wave front to propagate across the heart wall. Assume the wall thickness is 10 mm and the propagation speed is 0.2 m s^{-1}.

Problem 25. In an ECG recording, the width of one large square corresponds to 200 ms. A normal heart rate is between 60 and 100 beats min^{-1}. The heart rate is usually measured by counting the number of large squares between adjacent QRS complexes.

(a) How many large squares are there for a normal heart rate?

(b) In Fig. 7.30 determine the rate of the atria and of the ventricles.

Problem 26. Consider Lead II of the normal ECG in Fig. 7.23. The QRS wave and the T wave are both positive. Use a 1-dimensional model to convince yourself that the QRS complex and the T wave should have opposite polarities. Why then is the T wave inverted? Find a way to explain the inverted T wave by letting the action potential duration vary between epicardium (outside) and endocardium (inside). On which surface should the duration be longest?

Section 7.9

Problem 27. Ohm's law says that $\mathbf{j} = \sigma\mathbf{E}$. Draw what $\mathbf{j}$ and $\mathbf{E}$ look like (a) in a circuit consisting of a battery and a resistor; (b) for the current flowing when a nerve cell depolarizes.

Problem 28. Obtain the values for β for a cube of length a on a side, for a cylinder of radius a and length h, and for a sphere of radius a.

Problem 29. Show that Eq. 7.36a is the same as Eq. 6.51 by considering the interior of a single cell stretched along the x axis as in Fig. 6.28. Consider the charge in a small cylindrical region of axoplasm of length h and radius a, the cylindrical surface of which is surrounded by cell membrane. Show that the total charge Q within the axoplasm changes according to

$$\begin{aligned}\frac{\partial Q}{\partial t} &= \pi a^2 h \frac{\partial \rho_i}{\partial t} = C\frac{\partial v_m}{\partial t} + i_m \\ &= 2\pi a h\left(c_m \frac{\partial v_m}{\partial t} + j_m\right),\end{aligned}$$

and that this can be combined with Eq. 7.36a to give

$$\begin{aligned}c_m \frac{\partial v_m}{\partial t} + j_m &= \frac{\pi a^2 h}{2\pi a h}\sigma_i \frac{\partial^2 v_i}{\partial x^2} \\ &= \frac{\sigma_i a}{2}\frac{\partial^2 v_i}{\partial x^2},\end{aligned}$$

which is the same as Eq. 6.51, except that it is written in terms of σ_i, a, and h instead of a and r_i.

Problem 30. Clark and Plonsey (1968) solved Eq. 7.34 for a cylindrical axon of radius a using the following method. Assume that the potentials all vary in the z direction sinusoidally, for instance $v_m(z) = V\sin(kz)$, where V is a constant.

(a) Show that the intracellular and extracellular potentials can be written as

$$\begin{aligned}v_i &= AI_0(kr)\sin(kz) \\ v_o &= BK_0(kr)\sin(kz),\end{aligned} \tag{7.53}$$

where I_n and K_n are *modified Bessel functions* obeying the equation

$$\frac{1}{r}\frac{\partial}{\partial r}\left(r\frac{\partial v}{\partial r}\right) - \left(k^2 + \frac{n^2}{r^2}\right)v = 0.$$

(b) Determine the constants A and B in terms of V, using the following two boundary conditions: $v_m = v_i - v_o$, and $\sigma_i(\partial v_i/\partial r) = \sigma_o(\partial v_o/\partial r)$, both evaluated at $r = a$. You will need to use the Bessel function identities $dI_0(kr)/dr = kI_1(kr)$ and $dK_0(kr)/dr = -kK_1(kr)$. Clark and Plonsey used this result and Fourier analysis (Chap. 11) to determine v_i and v_o when they are not sinusoidal in z.

Problem 31. Starting with the bidomain equations, divide Eq. 7.44a by σ_{ix} and Eq. 7.44b by σ_{ox}. Now subtract one equation from the other. Under what conditions do the equations contain $v_m = v_i - v_o$ but not v_i and v_o individually?

Section 7.10

Problem 32. Verify Eq. 7.47.

Problem 33. Verify the values given for rheobase and chronaxie in Table 7.1 that are based on Table 6.1.

Problem 34. An approximation to the error function is given by Abramowitz and Stegun (1972)

$$\operatorname{erf}(x) \approx 1 - \Big(1 + 0.278393x + 0.230389x^2 + 0.000972x^3 + 0.078108x^4\Big)^{-4}, \quad x > 0.$$

Calculate $\operatorname{erf}(x)$ using this approximation for $x = 0, 0.5, 1.0, 2.0$ and ∞. Using trial and error, determine the value of x for which $\operatorname{erf}(x) = 0.5$. (See Eq. 7.50.)

Problem 35. Find the equivalent of Eq. 7.45 in terms of the charge required for the stimulation.

Problem 36. If the medium has a constant resistance, find the energy required for stimulation as a function of pulse duration.

Problem 37. A typical pacemaker electrode has a surface area of 10 mm^2. What is its resistance into an infinite medium if it is modeled as a sphere? If it is modeled as a disk? (You will have to use results from Chap. 6 and assign a value for σ_o.)

Problem 38. Equation 6.51 is the cable equation for a nerve axon. Assume that the axon membrane is passive ($j_m = g_m(v_i - v_o)$, where g_m is a constant).

(a) Express the equation in terms of v_m and v_o instead of v_i and v_o, where $v_m = v_i - v_o$.

(b) Divide the resulting equation by g_m, and then write the cable equation in terms of the time constant c_m/g_m and the length constant $1/\sqrt{2\pi a r_i g_m}$.

(c) Put all the terms containing v_m on the left side, and terms containing v_o on the right side. The resulting equation should look like Eq. 6.55, except for a new source term on the right side equal to $-\lambda^2 \partial^2 v_o/\partial x^2$. (Measure v_m with respect to resting potential so $v_r = 0$ in Eq. 6.55). The negative of this new term has been called the *activating function* (Rattay 1987). It is useful when studying electrical stimulation of nerves.

Problem 39. For this problem, use the activating function derived in Problem 38. Assume that λ and τ are negligibly small, so that v_m simply equals the activating function. Consider a point electrode in an infinite, homogeneous volume conductor at distance d from the axon. The extracellular potential is $v_o = (1/4\pi\sigma_o)\, I/r$.

(a) Calculate v_m as a function of position x along the axon ($x = 0$ is the closest position to the electrode).

(b) Assume that the axon will fire an action potential if v_m somewhere along the axon is greater than $V_{\text{threshold}}$. Calculate the ratio of the stimulation current I needed to excite the axon for a cathode (negative electrode) and an anode (positive electrode).

Problem 40. For this problem, use the activating function derived in Problem 38. An action potential can be excited if a stimulus depolarizes an axon to a value greater than $V_{\text{threshold}}$, and a propagating action potential can be blocked if a stimulus hyperpolarizes to a value of v_m less than $-V_{\text{block}}$ ($V_{\text{block}} > V_{\text{threshold}}$).

(a) For a cathodal electrode [$v_o = (1/4\pi\sigma_o)\, I/r$] calculate the ratio of the threshold current to the current needed to block propagation.

(b) Use two electrodes (one cathodal and one anodal) to design a stimulator that will result in one-way propagation along the axon (say, propagation only in the positive x direction, but blocked in the negative x direction). For an application of such electrodes during functional electrical stimulation, see Ungar et al. (1986).

Problem 41. For this problem, use the activating function derived in Problem 38, and block by hyperpolarization derived in Problem 40. The factor of λ^2 in the activating function implies that larger diameter axons are easier to stimulate than smaller diameter axons. Sometimes you want to excite the smaller fibers without the larger fibers (*physiological recruitment*). Describe qualitatively how you can use a single electrode and block in the hyperpolarized region to obtain physiological recruitment. For a more complete discussion, see Tai and Jiang (1994).

Problem 42. In *second degree heart block*, the wave front sometimes passes through the conduction system and sometimes does not. Qualitatively sketch the ECG for a heart with second degree block for at least five beats. Specifically include the case where every third wave is blocked. Include the P wave, the QRS wave, and the T wave.

Problem 43. During *sinus exit block* the SA node functions normally but the wave front fails to propagate from the SA node to the atria. Sketch five beats of an ECG with all beats normal except the third, which undergoes sinus exit block.

Problem 44. In *sick sinus syndrome* the SA node has a slow and erratic rate. The AV node and conduction system function properly. You plan to implant a pacemaker in the patient. Should it stimulate the atria or the ventricles? Why?

Problem 45. A patient with *intermittent heart block* has an AV node that functions normally most of the time with occasional episodes of block, lasting perhaps several hours. Design a pacemaker to treat the patient. Ideally, your design will not stimulate the heart when it is functioning normally. Describe

(a) whether you will stimulate the atria or ventricles

(b) which chambers you will monitor with a recording electrode

(c) what logic your pacemaker will use to determine when to stimulate. Your design may be similar to a *demand pacemaker* described in Jeffrey (2001, p. 132).

Problem 46. The Lapicque strength-duration (SD) curve is

$$\frac{i}{i_R} = 1 + \frac{t_C}{t},$$

the SD curve in terms of the error function is

$$\frac{i}{i_R} = \frac{1}{\text{erf}\left(\sqrt{0.228 t/t_C}\right)},$$

and the SD curve derived in Chap. 6 Problem 37 is

$$\frac{i}{i_R} = \frac{1}{1 - e^{-0.693 t/t_C}}.$$

(a) Plot all three curves for $0 < t/t_C < 5$. Use the equation in Problem 34 to evaluate the error function.
(b) Find approximations for each curve for $t/t_C \ll 1$. You may need the Taylor's series expansions $e^x \approx 1 + x$ and $\text{erf}(x) \approx 2x/\sqrt{\pi}$.
(c) Discuss the physical assumptions that were used to derive each curve.

Problem 47. Consider a pacemaker delivering a $2-$ mA, $1-$ V, $1-$ ms pulse every second. Pacemakers are often powered by a lithium-iodide battery that can deliver a total charge of 2 ampere hours.
(a) What is the energy per pulse?
(b) What is the average power?
(c) How long will the battery last?
(d) Your answer to (c) is an overestimate of battery lifetime, in part because the battery voltage begins to decline before all its charge has been delivered, and in part because the pacemaker circuitry requires a small, constant current. For this pacemaker, add a constant current drain of 5 μA and assume that the useful lifetime of the battery is over when 75 % of the total charge has been delivered. How long will the battery last in this case?

Problem 48. During stimulation of cardiac tissue through a small anode, the tissue under the electrode and in the direction perpendicular to the myocardial fibers is hyperpolarized, and adjacent tissue on each side of the anode parallel to the fiber direction is depolarized. Imagine that just before this stimulus pulse is turned on the tissue is refractory. The hyperpolarization during the stimulus causes the tissue to become excitable. Following the end of the stimulus pulse, the depolarization along the fiber direction interacts electrotonically with the excitable tissue, initiating an action potential *(break excitation)*. (This type of break excitation is very different than the break excitation analyzed on page 181.)
(a) Sketch pictures of the transmembrane potential distribution during the stimulus. Be sure to indicate the fiber direction, the location of the anode, the regions that are depolarized and hyperpolarized by the stimulus, and the direction of propagation of the resulting action potential.
(b) Repeat the analysis for break excitation caused by a cathode instead of an anode. For a hint, see Wikswo and Roth (2009).

Problem 49. The signal measured during optical mapping, V, is a weighted average of the transmembrane potential, $V_m(z)$, as a function of depth,

$$V = \int_0^\infty V_m(z) w(z) dz,$$

where $w(z)$ is a normalized weighting function. Suppose the incident light that produces the fluorescence decays with depth exponentially, with an optical length constant δ. Then $w(z) = \exp(-z/\delta)/\delta$. Often a shock will cause $V_m(z)$ to fall off exponentially with depth, $V_m(z) = V_0 \exp(-z/\lambda)$, where V_0 is the transmembrane potential at the tissue surface and λ is the electrical length constant (see Sect. 6.6.12).
(a) Perform the required integration to find an analytical expression for the optical signal, V, as a function of V_0, δ and λ.
(b) What is V in the case $\delta \ll \lambda$? Explain this result physically.
(c) What is V in the case $\delta \gg \lambda$? Explain this result physically.
(d) For which limit do you obtain an accurate measurement of the transmembrane potential at the surface, $V = V_0$?
For additional analysis, see Janks and Roth (2002).

Problem 50. Consider a two-dimensional sheet of cardiac tissue represented as a bidomain having unequal anisotropy ratios: $\sigma_{ix} = \sigma_{ex} = 0.2$, $\sigma_{iy} = 0.02$, and $\sigma_{ey} = 0.08$ S m^{-1}. Assume an insulated obstacle that current must go around is at the center of the sheet. At any point in the tissue, current will divide between the intracellular and extracellular spaces according to their conductivities, with a larger fraction of the current in the space with greater conductivity.
(a) If current is passed through the tissue in the x-direction, determine qualitatively where the tissue is depolarized and where it is hyperpolarized in the region surrounding the insulator. Recall, depolarization occurs where current passes from the intracellular into the extracellular space, and hyperpolarization where current passes from the extracellular into the intracellular space.
(b) Repeat this analysis if current is passed in the y-direction.
(c) What would be the transmembrane potential if the tissue had equal anisotropy ratios?
For additional analysis, see Langrill and Roth (2001).

Section 7.11

Problem 51. When measuring the EEG with electrodes distributed according to the 10–20 system, you obtain measurements of the potential difference between the ith electrode

($i = 1, \ldots, 20$) and the reference electrode ($i = 21$). Show that by computing the average reference $v_i^* = (v_i - v_{21}) - (1/20)\sum_{j=1}^{20}\left(v_j - v_{21}\right)$, the resulting values of v_i^* are independent of the reference potential v_{21}.

Problem 52. Consider a very simple model of the EEG: a dipole **p** pointing in the z direction at the center of a spherical conductor of radius R and conductivity σ_o. The potential v_o can be written as the sum of two terms: the potential of a dipole in an unbounded medium plus a potential that obeys Laplace's equation

$$v_o = \frac{p\cos\theta}{4\pi\sigma_o r^2} + Ar\cos\theta$$

where r and θ are in spherical coordinates, and A is an unknown constant.

(a) Use Appendix L to show that the second term in the expression for v_o obeys Laplace's equation.

(b) If the region outside the spherical conductor is air (an insulator), determine the value of A by using the boundary condition that the radial current at the surface of the sphere is zero.

(c) Calculate v_o as measured at the sphere surface ($r = R$), and determine by what factor v_o differs from what it would be in the case of an unbounded volume conductor.

Problem 53. Suppose you measure the EEG potential v_j at N locations $\mathbf{r}_j = (x_j, y_j, z_j)$, $j = 1, \cdots, N$. Assume v_j is produced by a dipole $\mathbf{p} = (p_x, p_y, p_z)$ located at the origin. Define

$$R = \sum_{j=1}^{N}\left[\frac{p_x x_j + p_y y_j + p_z z_j}{4\pi\sigma\left(x_j^2 + y_j^2 + z_j^2\right)^{3/2}} - v_j\right]^2,$$

which measures the least-squares difference between the data and the potential predicted by a single-dipole model. (Chap. 11 explores the least-squares method in greater detail.) The goal is to find the dipole components p_x, p_y, p_z that fit the data best (minimize R).

(a) Minimize R with respect to p_x (set $dR/dp_x = 0$) and find an equation relating p_x, p_y, and p_z.

(b) Repeat for p_y and p_z.

(c) Write the three equations in the form $\mathbf{Ap} = \mathbf{b}$, where **A** is a 3×3 matrix and **b** is a 3×1 vector. Find expressions for the components of **A** and **b**.

(d) If we had not assumed that we knew the location of the dipole, the problem would be much more difficult. Assume the dipole is at location $\mathbf{r}_p = (x_p, y_p, z_p)$. Modify R and then try to minimize it with respect to $\mathbf{r}_p$. Carry the calculation far enough to convince yourself that you must now solve nonlinear equations to determine $\mathbf{r}_p$. Press et al. (1992) discuss methods for making nonlinear least squares fits.

References

Abramowitz M, Stegun IA (1972) Handbook of mathematical functions with formulas, graphs and mathematical tables. U.S. Government Printing Office, Washington

Barold SS (1985) Modern cardiac pacing. Futura, Mount Kisco

Clark J, Plonsey R (1968) The extracellular potential field of a single active nerve fiber in a volume conductor. Biophys J 8:842–864

Delmar M, Sorgen PL (2009) Molecular organization and regulation of the cardiac gap junction channel connexin43. In Zipes DP, Jalife J (eds) Cardiac electrophysiology: from cell to bedside, 5th ed. Saunders, Philadelphia, pp 85–92

Dosdall DJ, Fast VG, Ideker RE (2009) Mechanisms of defibrillation. In Zipes DP, Jalife J (eds) Cardiac electrophysiology: from cell to bedside, 5th ed. Saunders, Philadelphia, pp 499–508

Geddes LA, Bourland JD (1985) The strength-duration curve. IEEE Trans Biomed Eng 32:458–459

George AL Jr (2009) Inheritable sodium channel diseases. In Zipes DP, Jalife J (eds) Cardiac electrophysiology: from cell to bedside, 5th ed. Saunders, Philadelphia, pp 29–42

Gray RA (2009) Rotors and spiral waves in the heart. In Zipes DP, Jalife J (eds) Cardiac electrophysiology: from cell to bedside, 5th ed. Saunders, Philadelphia, pp 349–359

Gulrajani RM (1998) Bioelectricity and biomagnetism. Wiley, New York

Harris JW, Stocker H (1998) Handbook of mathematics and computational science. Springer, New York

Henriquez CS (1993) Simulating the electrical behavior of cardiac tissue using the bidomain model. Crit Rev Biomed Eng 21(1):1–77

Henriquez CS, Ying W (2009) The bidomain model of cardiac tissue: from microscale to macroscale. In Efimov IR, Kroll MW, Tchou PJ (eds) Cardiac bioelectric therapy: mechanisms and practical implications. Springer, New York, pp 401–421

Hobbie RK The electrocardiogram as an example of electrostatics. Am J Phys 41:824–831

Janks DL, Roth BJ (2002) Averaging over depth during optical mapping of unipolar stimulation. IEEE Trans Biomed Eng 49:1051–1054

Janks DL, Roth BJ (2009) The bidomain theory of pacing. In Efimov IR, Kroll MW, Tchou PJ (eds) Cardiac bioelectric therapy: mechanisms and practical implications. Springer, New York, pp 63–83

Jeffrey K (2001) Machines in our hearts. Johns Hopkins University Press, Baltimore

Langrill DM, Roth BJ (2001) The effect of plunge electrodes during electrical stimulation of cardiac tissue. IEEE Trans Biomed Eng 48:1207–1211

Lapicque L (1909) Definition experimentale de l'excitabilite. Comptes Rendus Acad Sci 67(2):280–283

Lindemans FW, Denier van der Gong JJ (1978) Current thresholds and liminal size in excitation of heart muscle. Cardiovasc Res 12:477–485

Lopes da Silva FH (2008) The impact of EEG/EMG signal processing and modeling in diagnosis and management of epilepsy. IEEE Rev Biomed Eng 1:143–156

Luo CH, Rudy Y (1994) A dynamic model of the cardiac ventricular action potential. I. Simulations of ionic currents and concentration changes. Circ Res 74(6):1071–1096

Malmivuo J, Plonsey R (1995) Bioelectromagnetism. Oxford University Press, Oxford

Miller CE, Henriquez CS (1990) Finite element analysis of bioelectric phenomena. Crit Rev Biomed Eng 18(3):207–233

Mitrani RD, Klein LS, Rardon DP, Zipes DP, Miles WM (1995) Current trends in the implantable cardioverter–defibrillator. In Zipes DP, Jalife J (eds) Cardiac electrophysiology: from cell to bedside, 2nd ed. Saunders, Philadelphia, pp 1393–1403

Moses HW, Mullin JC (2007) A practical guide to cardiac pacing, 6th ed. Lippincott Williams and Wilkins, Philadelphia

Nunez PL, Srinivasan R (2005) Electric fields of the brain, 2nd ed. Oxford University Press, Oxford

Oudit GY, Backx PH (2004) Voltage-regulated potassium channels. In Zipes DP, Jalife J (eds) Cardiac electrophysiology: from cell to bedside, 5th ed. Saunders, Philadelphia, pp 29–42

Peckham PH, Knutson JS (2005) Functional electrical stimulation for neuromuscular applications. Phys Med Biol 47:R67–R84

Perlmutter JS, Mink JW (2006) Deep brain stimulation. Annu Rev Neurosci 29:229–257

Plonsey R (1969) Bioelectric Phenomena. McGraw-Hill, New York

Press WH, Teukolsky SA, Vetterling WT, Flannery BP (1992) Numerical Recipes in C: the art of scientific computing, 2nd ed., reprinted with corrections, 1995. Cambridge University Press, New York

Rardon DP, Miles WM, Zipes DP (2000) Atrioventricular block and dissociation. In Zipes DP, Jalife J (eds) Cardiac electrophysiology: from cell to bedside, 3rd ed. Saunders, Philadelphia, pp 451–459

Rattay F (1987) Ways to approximate current-distance relations for electrically stimulated fibers. J Theor Biol 125:339–349

Ripplinger CM, Efimov IR (2009) The virtual electrode hypothesis of defibrillation. In Efimov IR, Kroll MW, Tchou PJ (eds) Cardiac bioelectric therapy: mechanisms and practical implications. Springer, New York, pp 331–356

Rosenbaum DS, Jalife J (2001) Optical mapping of cardiac excitation and arrhythmias. Futura, Armonk

Roth BJ (1992) How the anisotropy of the intracellular and extracellular conductivities influences stimulation of cardiac muscle. J Math Biol 30:633–646

Roth BJ (1997) Electrical conductivity values used with the bidomain model of cardiac tissue. IEEE Trans Biomed Eng 44:326–328

Rudy Y, Burnes JE (1999) Noninvasive electrocardiographic imaging. Ann Noninvasive Electrocardiol 4(3):340–359

Stanley PC, Pilkington TC, Morrow MN (1986) The effects of thoracic inhomogeneities on the relationship between epicardial and torso potentials. IEEE Trans Biomed Eng 33(3):273–284

Tai C, Jiang D (1994) Selective stimulation of smaller fibers in a compound nerve trunk with single cathode by rectangular current pulses. IEEE Trans Biomed Eng 41:286–291

Trayanova N, Plank G (2009) The bidomain model of defibrillation. In Efimov IR, Kroll MW, Tchou PJ (eds) Cardiac bioelectric therapy: mechanisms and practical implications. Springer, New York, pp 85–110

Trayanova N, Henriquez CS, Plonsey R (1990) Limitations of approximate solutions for computing extracellular potential of single fibers and bundle equivalents. IEEE Trans Biomed Eng 37(1):22–35

Ungar IJ, Mortimer JT, Sweeney JD (1986) Generation of unidirectionally propagating action potentials using a monopolar electrode cuff. Ann Biomed Eng 14:437–450

Voorhees CR, Voorhees WD III, Geddes LA, Bourland JD, Hinds M (1992) The chronaxie for myocardium and motor nerve in the dog with chest-surface electrodes. IEEE Trans Biomed Eng 39(6):624–628

Watanabe A, Grundfest H (1961) Impulse propagation at the septal and commissural junctions of crayfish lateral giant axons. J Gen Physiol 45:267–308

Wikswo JP, Roth BJ (2009) Virtual electrode theory of pacing. In Efimov IR, Kroll MW, Tchou PJ (eds) Cardiac bioelectric therapy: mechanisms and practical implications. Springer, New York, pp 283–330

Zeng F-G, Rebscher S, Harrison W, Sun X, Feng H (2008) Cochlear implants: system design, integration and evaluation. IEEE Rev Biomed Eng 1:115–142